AWARD NUMBER: W81XWH-10-1-0425

TITLE: Improve T Cell Therapy in Neuroblastoma

PRINCIPAL INVESTIGATOR: Dotti, G ianpietro, MD

CONTRACTING ORGANIZATION: Baylor College of Medicine
Houston, TX 77030

REPORT DATE: September 2015

TYPE OF REPORT: Final

PREPARED FOR: U.S. Army Medical Research and Materiel Command
Fort Detrick, Maryland 21702-5012

REPORT DOCUMENTATION PAGE

Form Approved
OMB No. 0704-0188

1. REPORT DATE	2. REPORT TYPE	3. DATES COVERED
September 2015	Final	1Jul2010 - 30Jun2015

4. TITLE AND SUBTITLE

Improve T Cell Therapy in Neuroblastoma

5a. CONTRACT NUMBER
W81XWH-10-1-0425

5b. GRANT NUMBER

5c. PROGRAM ELEMENT NUMBER

6. AUTHOR(S)

Dotti, Gianpietro, MD

E-Mail: gdotti@bcm.tmc.edu

5d. PROJECT NUMBER

5e. TASK NUMBER

5f. WORK UNIT NUMBER

7. PERFORMING ORGANIZATION NAME(S) AND ADDRESS(ES)

Baylor College of Medicine
One Baylor Plaza
Houston, TX 77030

8. PERFORMING ORGANIZATION REPORT NUMBER

9. SPONSORING / MONITORING AGENCY NAME(S) AND ADDRESS(ES)
U.S. Army Medical Research and Materiel Command
Fort Detrick, Maryland 21702-5012

10. SPONSOR/MONITOR'S ACRONYM(S)

11. SPONSOR/MONITOR'S REPORT NUMBER(S)

12. DISTRIBUTION / AVAILABILITY STATEMENT
Approved for Public Release; Distribution Unlimited

13. SUPPLEMENTARY NOTES

14. ABSTRACT

Neuroblastoma (NB) is the most common malignant extracranial tumor of childhood. Since NB appears susceptible to immunotherapies that include monoclonal antibodies and T-cell immune responses elicited by tumor vaccine, we have combined the beneficial effects of both humoral and cell-mediated components of the anti tumor response. We demonstrated indeed that adoptive transfer of Epstein-Barr-virus (EBV)-specific cytotoxic T lymphocytes (EBV-CTLs) genetically modified to express a chimeric antigen receptor (CAR-GD2) targeting the GD2 antigen expressed by neuroblasts persist in the peripheral blood and induce objective tumor responses (including complete remissions). We will now augment the expansion and survival of CAR-GD2 modified EBV-CTLs by coexpressing the IL-7Rα that restores their capacity to respond to homeostatic IL-7. We will also enhance the capacity of these cells to invade solid tumor masses by expressing heparanase (HPSE) that disrupts the non-cellular stromal elements of NB. Experiments will be conducted in vitro and in vivo in a xenograft mouse model.

15. SUBJECT TERMS
Neuroblastoma, immunotherapy, chimeric antigen receptor, GD2 antigen, heparanase, regulatory T cells, tumor stroma.

16. SECURITY CLASSIFICATION OF:			17. LIMITATION OF ABSTRACT	18. NUMBER OF PAGES	19a. NAME OF RESPONSIBLE PERSON
a. REPORT	b. ABSTRACT	c. THIS PAGE			USAMRMC
U	U	U	UU	30	19b. TELEPHONE NUMBER *(include area code)*

Table of Contents

1. INTRODUCTION

The overall goal of this project is to develop novel immunotherapy strategies to improve the clinical outcome of patients with neuroblastoma.

2. KEYWORD

Neuroblastoma, adoptive T cell immunotherapy, chimeric antigen receptor, tumor microenvironment.

3. OVERALL PROJECT SUMMARY

In our recent Phase I study we found that the adoptive transfer of Epstein-Barr-virus (EBV)-specific cytotoxic T lymphocytes (EBV-CTLs) genetically modified to express a chimeric antigen receptor (CAR-GD2) targeting the GD2 antigen expressed by neuroblasts, can persist in the peripheral blood for 6 weeks and induce objective tumor responses (including complete remission) or tumor necrosis in 4/8 subjects with refractory/relapsed NB[1]. Although encouraging, this study also revealed that the signal from the transgenic CTLs progressively declined over time in the majority of patients[1;2] suggesting that the anti tumor effects of these cells could be augmented by prolonging the survival and effector function of the transgenic CTLs, for example by restoring their responsiveness to homeostatic cytokines such as IL-7[3] and inducing a robust $CD8^+$ T cell memory response[4]. Our second approach aims to disrupt the non-cellular stromal elements of NB that may impede access to CAR-modified EBV-CTLs. The ability of tumor-specific CTLs to cross tumor blood vessels is crucial for reaching the tumor cells. Leukocyte extravasation is highly dependent upon the degradation of the components of the subendothelial basement membrane (SBM) and the extracellular matrix (ECM) such as heparan sulfate proteoglycans (HSPGs), fibronectin and collagen[5]. Heparanase (HPSE) is the only known mammalian endoglycosidase degrading HSPGs at distinct HS intra-chain sites[5;6]. Although HPSE is expressed in activated $CD4^+$ lymphocytes, neutrophils, monocytes and B lymphocytes[5;7;8] we have found it to be deficient in cultured T cells and EBV-CTLs.

4. KEY RESEARCH ACCOMPLISHMENT

In Task 1 we proposed to co-express CAR-GD2 and IL-7Rα in EBV-CTLs to improve their expansion and anti tumor effects in response to IL-7, whilst avoiding the expansion of regulatory T cells (Treg) (time frame months 1-24).

- We optimized the methodology to expand *ex vivo* fully functional regulatory T cells (Tregs) (as assessed in a model of graft versus host disease (GvHD)) that can be used for the experiments *in vitro* and *in vivo* proposed in this task of the proposal. The results of these experiments have been published in manuscript #1 listed in the Reportable Outcome section (Chakraborty R et al. Haematologica. 2013 Apr;98(4):533-7).
- We formally demonstrated that our proposed hypothesis that the genetic manipulation of EBV-CTLs to express CAR-GD2 and IL-7Rα renders these cells resistant to the inhibitory effects of Tregs *in vitro* and *in vivo* in a xenograft neuroblastoma model is correct. The results of these experiments have been summarized in manuscript #2 and #3 listed in the Reportable Outcome section (Perna SK et al Clin Cancer Res. Clin Cancer Res. 2014 Jan 1;20(1):131-9. Highlited article.

This task has been completed and the results reported in three publications:

1 Chakraborty R, Mahendravada A, Perna SK, Rooney CM, Heslop HE, Vera JF, Savoldo B, Dotti G. Robust and cost effective expansion of human regulatory T cells highly functional in a xenograft model of graft versus host disease. Haematologica. 2013 Apr;98(4):533-7.

2 Perna SK, Pagliara D, Mahendravada A, Liu H, Brenner M, Savoldo B and Dotti G. Interleukin-7 mediates selective expansion of tumor-redirected cytotoxic T lymphocytes without enhancement of regulatory T-cell inhibition. Clin Cancer Res. Clin Cancer Res. 2014 Jan 1;20(1):131-9. Highlited article.

3 Perna SK, Savoldo B, Dotti G. Genetic modification of cytotoxic T lymphocytes to express cytokine receptors. Methods Mol Biol. 2014;1139:189-200.

Task 2. To evaluate the contribution of IL-7Rα ligation and co-stimulation from viral-infected target cells on the development of long-lived memory CAR-GD2-mofied EBV-CTLs in a humanized SCID mouse model previously engrafted with human hematopoietic stem cells (time frame months 12-48).

During the no cost extension period we have completed the *in vivo* experiments and demonstrated that aAPCs can be used to boost CAR-redirected CTLs *in vivo* in a xenograft model of neuroblastoma. In summary we have found that

- aAPCs expressing pp65 and OX40L and CD40L enhance the anti-neuroblastoma activity of CTLs expressing the GD2-specific CAR in two xenograft mouse models of neuroblastoma.

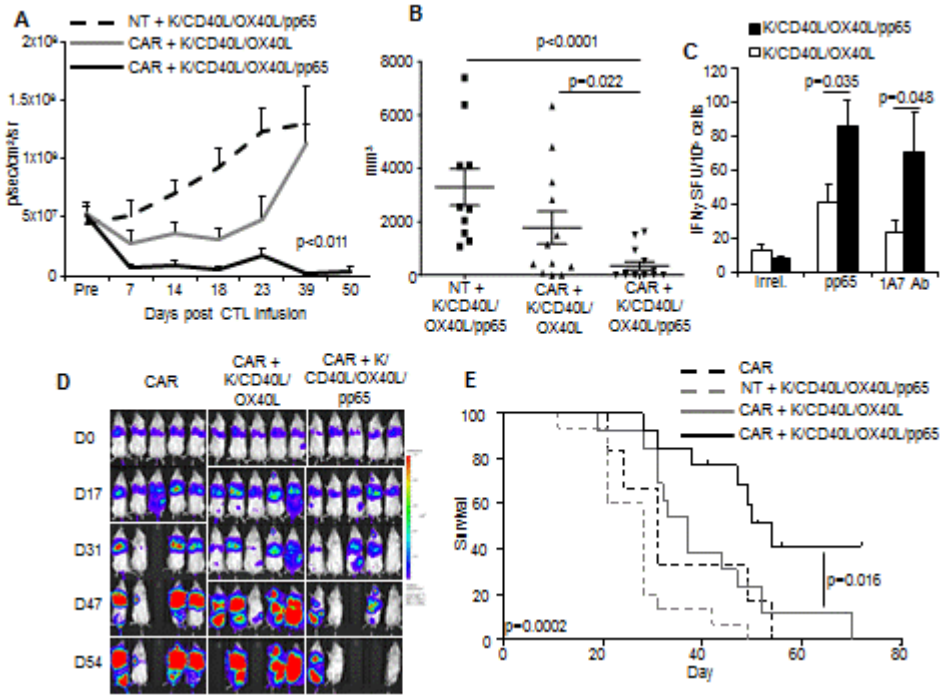

Figure 1: Vaccination with K562-derived whole-cell vaccine expressing CMV-pp65, CD40L and OX40L enhances antitumor effects of CAR-CMV-CTLs *in vivo*. Panel A. NOG/SCID/$\gamma_c^{-/-}$ mice engrafted i.p. with the neuroblastoma cell line CHLA-255 labeled with firefly luciferase were infused i.p. with control or CAR-CMV-CTLs and vaccinated. The graph summarizes tumor bioluminescence. Summary of CMV-CTL line prepared from 4 donors: 15 mice (control CMV-CTLs plus K/CD40L/pp65 and K/OX40L/pp65), 17 mice (CAR-CMV-CTLs plus K/CD40L and K/OX40L) and 17 mice (CAR-CMV-CTLs plus K/CD40L/pp65 and K/OX40L/pp65) were used per group. **Panel B**. Mice euthanized were analyzed for the presence of macroscopic tumors. The graph summarizes the volume of the tumor collected in the different groups. **Panel C**. Enumeration of the CMV-CTLs in the isolated human CD45$^+$ cells from the spleen as assessed by IFNγ ELISpot in response to CMV-pp65 and irrelevant pepmixes or the 1A7 Ab that cross-links the CAR-GD2. Data represent mean ± SD. **Panel D**. Mice were inoculated i.v. with the GD2$^+$ lung carcinoma cell line A459 labeled with Firefly luciferase. Mice were then infused i.v. with control or CAR-CMV-CTLs and vaccinated. Tumor bioluminescence was then measured overtime. The graph is representative of one of 4 experiments using CMV-CTLs from 4 donors. **Panel E**. Kaplan-Meier analysis of tumor-bearing mice. Summary of CMV-CTL lines prepared from 4 donors: 15 mice (control CMV-CTLs plus K/CD40L/pp65 and K/OX40L/pp65), 13 mice (CAR-CMV-CTLs plus K/CD40L and K/OX40L), 13 mice (CAR-CMV-CTLs plus K/CD40L/pp65 and K/OX40L/pp65) and 8 mice (CAR-CMV-CTLs alone) were used per group.

- The inclusion of the safety switch iC9 allows the rapid elimination of the aAPCs *in vivo* increasing the safety of the proposed approach.

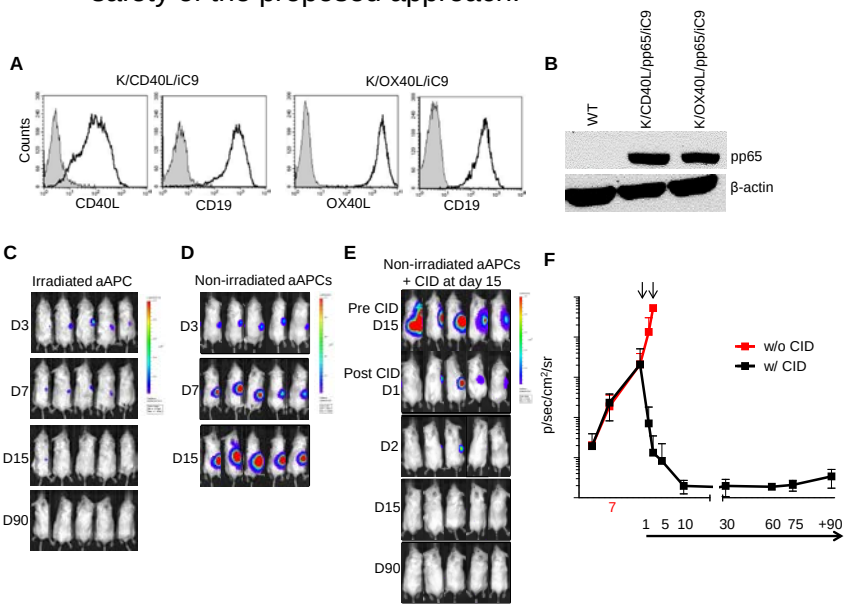

Figure 2: Activation of the *iC9* suicide gene eliminates engrafted K562-derived whole-cell vaccine *in vivo*. Panel A. Characterization of the clones by flow cytometry analysis. Gray areas indicate wild type K562 cells. **Panel B.** Western blot showing the expression of CMV-pp65 in the clones expressing the *iC9* transgene. **Panels C and D.** NOG/SCID/$\gamma_c^{-/-}$ mice were inoculated subcutaneously with irradiated (**C**) or non-irradiated (**D**) K562-derived whole-cell vaccine expressing the *iC9* gene and labeled with an enhanced firefly luciferase. Tumor growth was measured by *in vivo* imaging. **Panel E**. Effects of the administration of the chemical inducer of dimerization (CID) AP4076 on the growth of engineered vaccine.

This task has been completed and the results reported in a publication:

4 Caruana I, Weber G, Ballard BC, Wood MS, Savoldo B, **Dotti G**. K562-Derived Whole-Cell Vaccine Enhances Antitumor Responses of CAR-Redirected Virus-Specific Cytotoxic-T Lymphocytes in vivo. Clin Cancer Res. 2015 Jul 1;21(13):2952-62.

Task 3: To co-express CAR-GD2 and HPSE in EBV-CTLs and determine the consequent modulation of NB tissue infiltration and killing (time frame 1-48).

During the no cost extension period we have completed the *in vitro* and *in vivo* experiments as requested by the reviewers of the manuscript we have submitted to Nature Medicine. We have completed all the experiments. In particular we have demonstrated that:

- Demonstration that the constitutive expression of HPSE is equally down regulated in T cells cultured using different experimental conditions such as: T cell expansion in human AB serum rather than FBS; presence of IL-7/IL-15 cytokines rather than IL-2 or high doses of IL-2 rather than low doses of IL-2.

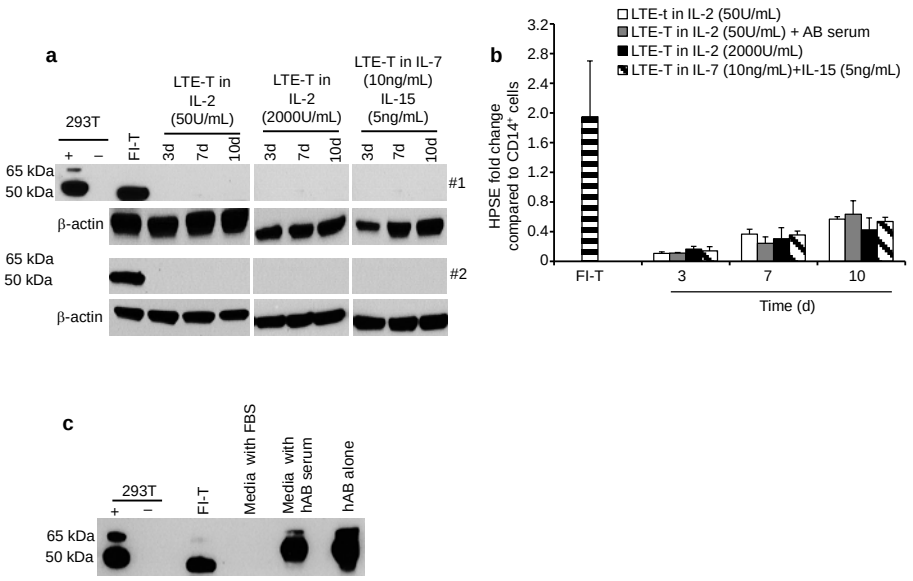

Figure 3. HPSE down regulation in LTE-T cells is not caused by specific culture conditions. T lymphocytes were activated with immobilized OKT3 (1 µg ml) and anti-CD28 (1 µg ml) Abs, and then expanded in complete medium supplemented with either 10% FBS and either IL-2 (50 U mL) or IL-2 (2000 U mL) or IL-7 (10 ng mL) and IL-15 (5 ng mL) twice a week. Expression of HPSE was assessed in cell lysates by western blot (**a**) and qRT-PCR (**b**) at day 3, 7 and 10 after T-cell activation. (**a**,**b**) Illustrate data from 2 and 4 donors, respectively. We also assessed whether the presence of FBS in the culture media affected HPSE expression. We removed FBS from the media and used human AB serum (5%). *HPSE* mRNA was down regulated also in the presence if hAB serum as assessed by qRT-PCR (**b**). Western blot is not informative in the presence of hAB serum since, as illustrated in (**c**), hAB serum contains HPSE.

- Demonstration that other matrix-metalloproteases can also be downregulated.

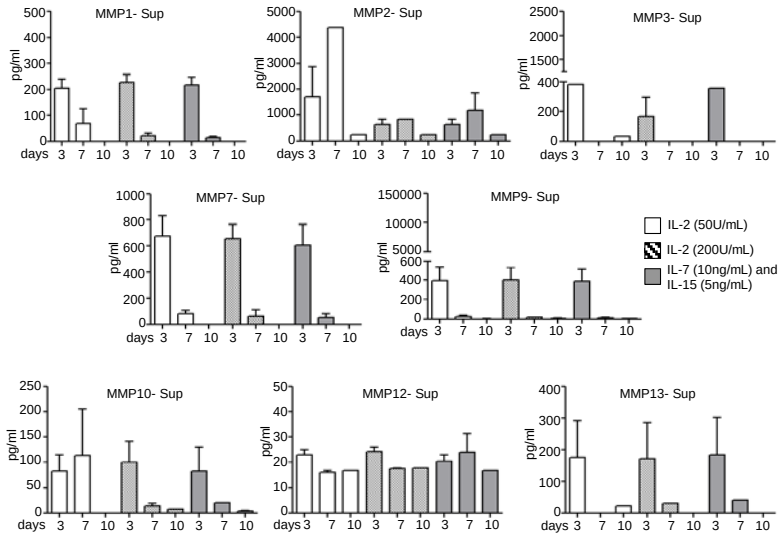

Figure 4. Analysis of matrix metallo-proteases (MMPs) in T lymphocytes. Supernatants were collected from T lymphocytes obtained 3, 7 and 10 days after activation with OKT3 and anti-CD28 mAbs in the presence of IL-2 (50 U mL), or IL-2 (2000 U mL) or IL-7 and IL-15 (10 ng mL and 5 ng mL, respectively). Detection of MMs was performed using Milliplex Map kit (Millipore). Data summarizes means ± SD of 3 donors.

- Demonstration that T cells expressing a different CAR targeting another antigen expressed by solid tumor show similar outcome as observed for the GD2 antigen expressed by neuroblastoma.

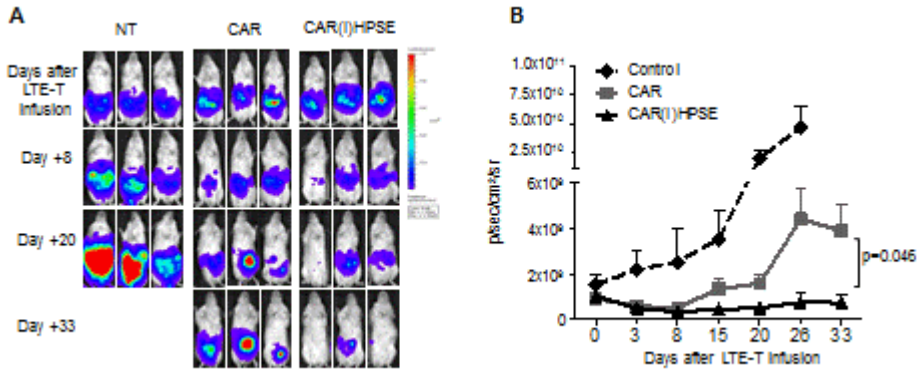

Figure 5. Co-expression of *HPSE* in CSPG4-specific CAR-modified LTE-T cells improves the antitumor effects in an aggressive melanoma model. NSG mice were inoculated intraperitoneally with $5x10^5$ SEMNA cells ($CSPG4^+$ melanoma) resuspended in Matrigel and labelled with firefly luciferase. By day 2, mice were infused intraperitoneally with control, CAR.CSPG4 (4-1BB costimulation) or CAR.CSPG4 (4-1BB costimulation)(I)HPSE LTE-T cells (10^7 cells)[2]. For these experiments, LTE-T cells were cultured in IL-7 and IL-15 since these cytokines prolong the persistence of LTE-T cells in NSG mice[3]. (**a**) Illustrates tumor growth in 3 representative animals per group, as assessed by IVIS imaging. (**b**) Shows the summary of the tumor bioluminescence of 2 experiments (8 mice per group using 2 donors).

This task has been completed and the results reported in a publication:

5 Caruana I, Savoldo B, Hoyos V, Weber G, Liu H, Kim ES, Ittmann MM, Marchetti D, **Dotti G**. Heparanase promotes tumor infiltration and antitumor activity of CAR-redirected T lymphocytes. Nat Med. 2015 May;21(5):524-529.

5. CONCLUSIONS

From Task 1 we have demonstrated that our proposed approach to modulate the IL-7/IL-7Rα receptor axis in EBV-CTLs redirected with a CAR that targets the GD2 antigen expressed by neuroblastoma promotes the expansion of these cells in response to IL-7 without favoring the expansion of Tregs. This is highly relevant since this strategy will support better expansion of these cells in patients with neuroblastoma without promoting Tregs that are particularly abundant in these patients and significantly contribute in blocking immune responses.

From Task 2 we have demonstrated that artificial antigen presenting cells aAPCs that can boost virus-specific CTLs expressing a CAR-GD2 specific and enhance their antitumor activity in neuroblastoma.

From task 3 we have discovered a major deficiency of T cells used for adoptive immunotherapy. These cells lack the expression of a key enzyme – HPSE – that drives their infiltration of the stroma of solid tumors. We also demonstrated that this defect can be repaired enhancing the capacity of these cells to eliminate neuroblastoma cells in a relevant xenogenic mouse model. This approach may also play a crucial role in improving the clinical efficacy of CAR-redirected CTLs.

6. PUBBLICATIONS

6 Chakraborty R, Mahendravada A, Perna SK, Rooney CM, Heslop HE, Vera JF, Savoldo B, Dotti G. Robust and cost effective expansion of human regulatory T cells highly functional in a xenograft model of graft versus host disease. Haematologica. 2013 Apr;98(4):533-7.

7 Perna S, Pagliara D, Mahendravada A, Liu H, Brenner M, Savoldo B and Dotti G.Interleukin-7 mediates selective expansion of tumor-redirected cytotoxic T lymphocytes without enhancement of regulatory T-cell inhibition. Clin Cancer Res. 2014 Jan 1;20(1):131-9. Highlited article.

8 Perna SK, Savoldo B, Dotti G. Genetic modification of cytotoxic T lymphocytes to express cytokine receptors. Methods Mol Biol. 2014;1139:189-200

9 Arber C, Abhyankar H, Heslop H, Brenner MK, Dotti G, Savoldo B. The immunogenicity of virus-derived 2A sequences in immunocompetent individuals. Gene Therapy 2013 Sep;20(9):958-62.

10 Caruana I, Weber G, Ballard BC, Wood MS, Savoldo B, **Dotti G**. K562-Derived Whole-Cell Vaccine Enhances Antitumor Responses of CAR-Redirected Virus-Specific Cytotoxic-T Lymphocytes in vivo. Clin Cancer Res. 2015 Jul 1;21(13):2952-62.

11 Caruana I, Savoldo B, Hoyos V, Weber G, Liu H, Kim ES, Ittmann MM, Marchetti D, **Dotti G**. Heparanase promotes tumor infiltration and antitumor activity of CAR-redirected T lymphocytes. Nat Med. 2015 May;21(5):524-529.

Other publications during the last period

12 Ando M, Hoyos V, Yagyu S, Tao W, Ramos CA, **Dotti G**, Brenner MK, Bouchier-Hayes L.Bortezomib sensitizes non-small cell lung cancer to mesenchymal stromal cell-delivered inducible caspase-9-mediated cytotoxicity. Cancer Gene Ther. 2014 Nov;21(11):472-82.

13 Gargett T, Fraser CK, **Dotti G**, Yvon ES, Brown MP. BRAF and MEK Inhibition Variably Affect GD2-specific Chimeric Antigen Receptor (CAR) T-Cell Function In Vitro. J Immunother. 2015 Jan;38(1):12-23.

14 Arber C, Feng X, Abhyankar H, Romero E, Wu MF, Heslop HE, Barth P, Dotti G, Savoldo B. Survivin-specific T cell receptor targets tumor but not T cells. J Clin Invest. 2015 Jan 2;125(1):157-68.

15 Casucci M, Hawkins RE, **Dotti G**, Bondanza A. Overcoming the toxicity hurdles of genetically targeted T cells. Cancer Immunol Immunother. 2015 Jan;64(1):123-30.

16 Sun J, Huye LE, Lapteva N, Mamonkin M, Hiregange M, Ballard B, Dakhova O, Raghavan D, Durett AG, Perna SK, Omer B, Rollins LA, Leen AM, Vera JF, **Dotti G**, Gee AP, Brenner MK, Myers DG, Rooney CM. Early transduction produces highly functional chimeric antigen receptor-modified virus-specific T-cells with central memory markers: a Production Assistant for Cell Therapy (PACT) translational application. J Immunother Cancer. 2015 in press

17 Ahmed N, Brawley VS, Hegde M, Robertson C, Ghazi A, Gerken C, Liu E, Dakhova O, Ashoori A, Corder A, Gray T, Wu MF, Liu H, Hicks J, Rainusso N, **Dotti G**, Mei Z, Grilley B, Gee A, Rooney CM, Brenner MK, Heslop HE, Wels WS, Wang LL, Anderson P, Gottschalk S. Human Epidermal Growth Factor Receptor 2 (HER2)-Specific Chimeric Antigen Receptor-Modified T Cells for the Immunotherapy of HER2-Positive Sarcoma. J Clin Oncol. 2015 May 20;33(15):1688-96.

18 Ninomiya S, Narala N, Huye L, Yagyu S, Savoldo B, **Dotti G**, Heslop HE, Brenner MK, Rooney CM, Ramos CA Tumor indoleamine 2,3-dioxygenase (IDO) inhibits CD19-CAR T cells and is downregulated by lymphodepleting drugs. Blood. 2015 Jun 18;125(25):3905-16.

19 Nishio N, **Dotti G**. Oncolytic virus expressing RANTES and IL-15 enhances function of CAR-modified T cells in solid tumors. Oncoimmunology. 2015 Mar 6;4(2).

20 Zhou X, **Dotti G**, Krance RA, Martinez CA, Naik S, Kamble RT, Durett AG, Dakhova O, Savoldo B, Di Stasi A, Spencer DM, Lin YF, Liu H, Grilley BJ, Gee AP, Rooney CM, Heslop HE, Brenner MK. Inducible caspase-9 suicide gene controls adverse effects from alloreplete T cells after haploidentical stem cell transplantation. Blood. 2015 Jun 25;125(26):4103-13

21 Hoyos V, Del Bufalo F, Yagyu S, Ando M, **Dotti G**, Suzuki M, Bouchier-Hayes L, Alemany R, Brenner MK. Mesenchymal stromal cells for linked delivery of oncolytic and apoptotic adenoviruses to non-small cell lung cancers. Mol Ther. 2015 Jun 18. doi: 10.1038/mt.2015.110. [Epub ahead of print]

22 Wang Y, Geldres C, Ferrone S, **Dotti G**. Chondroitin sulfate proteoglycan 4 as a target for chimeric antigen receptor-based T-cell immunotherapy of solid tumors. Expert Opin Ther Targets. 2015 Jul 18:1-12. [Epub ahead of print]

23 **Gianpietro Dotti**. Control of leukemia relapse after allogeneic hematopoietic stem cell transplantation: integrating transplantation with genetically modified T cell therapies. Current Opinion in Hematology. 2015. In press

7. INVENTION, PATENTS AND LICENCERS

A provisional patent has been issued by Baylor College of Medicine on the discovery reported in Task 3.

8. REPORTABLE OUTCOMES

- We have demonstrated that our proposed approach to modulate the IL-7/IL-7Rα receptor axis in EBV-CTLs redirected with a CAR that targets the GD2 antigen expressed by neuroblastoma promotes the expansion of these cells in response to IL-7 without favoring the expansion of Tregs. This is highly relevant since this strategy will support better expansion of these cells in patients with neuroblastoma without promoting Tregs that are particularly abundant in these patients and significantly contribute in blocking immune responses.

- We have generated artificial antigen presenting cells aAPCs that can boost virus-specific CTLs expressing a CAR-GD2 specific. We will continue to validate these aAPCs in a xenograft model of neuroblastoma. If the experiments are successful, this represents another relevant strategy that can be added to the one described in Task 1 to promote the survival on CAR-redirected CTLs in patients with neuroblastoma.

- We have discovered a major deficiency of T cells used for adoptive immunotherapy. These cells lack the expression of a key enzyme – HPSE – that drives their infiltration of the stroma of solid tumors. We also demonstrate that this defect can be repaired enhancing the capacity of these cells to eliminate neuroblastoma cells in a relevant xenogenic mouse model. This approach may also play a crucial role in improving the clinical efficacy of CAR-redirected CTLs.

9. OTHER ACHIEVMENTS: nothing to report

10. REFERENCES

Reference List

1. Pule MA, Savoldo B, Myers GD et al. Virus-specific T cells engineered to coexpress tumor-specific receptors: persistence and antitumor activity in individuals with neuroblastoma. Nat.Med. 2008;14:1264-1270.

2. Louis CU, Savoldo B, Dotti G et al. Antitumor activity and long-term fate of chimeric antigen receptor-positive T cells in patients with neuroblastoma. Blood 2011;118:6050-6056.

3. Vera J, Savoldo B, Vigouroux S et al. T lymphocytes redirected against the kappa light chain of human immunoglobulin efficiently kill mature B lymphocyte-derived malignant cells. Blood 2006;108:3890-3897.

4. Buentke E, Mathiot A, Tolaini M et al. Do CD8 effector cells need IL-7R expression to become resting memory cells? Blood 2006;108:1949-1956.

5. Parish CR. The role of heparan sulphate in inflammation. Nat.Rev.Immunol. 2006;6:633-643.

6. Edovitsky E, Elkin M, Zcharia E, Peretz T, Vlodavsky I. Heparanase gene silencing, tumor invasiveness, angiogenesis, and metastasis. J.Natl.Cancer Inst. 2004;96:1219-1230.

7. de Mestre AM, Staykova MA, Hornby JR, Willenborg DO, Hulett MD. Expression of the heparan sulfate-degrading enzyme heparanase is induced in infiltrating CD4+ T cells in experimental autoimmune encephalomyelitis and regulated at the level of transcription by early growth response gene 1. J.Leukoc.Biol. 2007;82:1289-1300.

8. de Mestre AM, Soe-Htwe T, Sutcliffe EL et al. Regulation of mouse Heparanase gene expression in T lymphocytes and tumor cells. Immunol.Cell Biol. 2007;85:205-214.

9. Geldres C, Savoldo B, Hoyos V et al. T lymphocytes redirected against the chondroitin sulfate proteoglycan-4 control the growth of multiple solid tumors both in vitro and in vivo. Clin.Cancer Res. 2014;20:962-971.

11. APPENDICES

Published OnlineFirst February 17, 2015; DOI: 10.1158/1078-0432.CCR-14-2998

Cancer Therapy: Preclinical

Clinical Cancer Research

K562-Derived Whole-Cell Vaccine Enhances Antitumor Responses of CAR-Redirected Virus-Specific Cytotoxic T Lymphocytes *In Vivo*

Ignazio Caruana[1], Gerrit Weber[1], Brandon C. Ballard[1], Michael S. Wood[1], Barbara Savoldo[1,2], and Gianpietro Dotti[1,3,4]

Abstract

Purpose: Adoptive transfer of Epstein–Barr virus (EBV)–specific and cytomegalovirus (CMV)-specific cytotoxic T cells (CTL) genetically modified to express a chimeric antigen receptor (CAR) induces objective tumor responses in clinical trials. *In vivo* expansion and persistence of these cells are crucial to achieve sustained clinical responses. We aimed to develop an off-the-shelf whole-cell vaccine to boost CAR-redirected virus-specific CTLs *in vivo* after adoptive transfer. As proof of principle, we validated our vaccine approach by boosting CMV-specific CTLs (CMV-CTLs) engineered with a CAR that targets the GD2 antigen.

Experimental Design: We generated the whole-cell vaccine by engineering the K562 cell line to express the CMV-pp65 protein and the immune stimulatory molecules CD40L and OX40L. Single-cell–derived clones were used to stimulate CMV-CTLs *in vitro* and *in vivo* in a xenograft model. We also assessed whether the *in vivo* boosting of CAR-redirected CMV-CTLs with the whole-cell vaccine enhances the antitumor responses. Finally, we addressed potential safety concerns by including the inducible safety switch caspase9 (*iC9*) gene in the whole-cell vaccine.

Results: We found that K562-expressing CMV-pp65, CD40L, and OX40L effectively stimulate CMV-specific responses *in vitro* by promoting antigen cross-presentation to professional antigen-presenting cells (APCs). Vaccination also enhances antitumor effects of CAR-redirected CMV-CTLs in xenograft tumor models. Activation of the *iC9* gene successfully induces growth arrest of engineered K562 implanted in mice.

Conclusions: Vaccination with a whole-cell vaccine obtained from K562 engineered to express CMV-pp65, CD40L, OX40L and *iC9* can safely enhance the antitumor effects of CAR-redirected CMV-CTLs. *Clin Cancer Res; 21(13); 2952–62. ©2015 AACR.*

Introduction

Chimeric antigen receptor (CAR)–redirected T lymphocytes mediate HLA-independent cytotoxic activity against a variety of human malignancies in preclinical models (1, 2). In clinical trials, adoptively transferred CAR-T lymphocytes induce durable tumor regressions when CAR-T cells expand and persist *in vivo* (3, 4). Proliferation and survival of CAR-T cells are strictly dependent on their adequate costimulation (3, 5, 6). Antigen-presenting cells (APC), such as dendritic cells, that present MHC-restricted antigen epitopes to the T-cell receptor, and express costimulatory molecules in a spatially and temporally coordinated fashion, provide the most physiologic T-cell costimulation (7). We previously hypothesized that engrafting CARs in virus-specific cytotoxic T cells (VsCTLs), such as Epstein–Barr virus (EBV)-CTLs or cytomegalovirus (CMV)-CTLs, can recapitulate a physiologic T-cell costimulation of CAR-engineered T cells. VsCTLs expressing a CAR are indeed "dual specific" and can receive a proper costimulation by APCs processing and presenting viral epitopes to VsCTL native virus-specific T-cell receptors, while the CAR expression redirects their cytotoxic activity toward tumor cells (8–10).

We validated this strategy in clinical trials, in both the autologous and allogeneic settings. In patients with neuroblastoma, we described how autologous EBV-CTLs engineered with a first-generation (encoding only the ζ chain moiety) GD2-specific CAR have better initial engraftment compared with autologous polyclonal activated T lymphocytes expressing the same CAR (11). In the context of the allogeneic stem cell transplant, we also showed that donor-derived EBV-CTLs and CMV-CTLs engrafted with a second-generation CD19-specific CAR, encoding both the CD28 and ζ chain moieties, can produce antitumor and antiviral activity without causing graft versus host disease (12). However, there were some limitations in both autologous and allogeneic settings. For instance, in patients with neuroblastoma, although detectable long-term, autologous GD2-specific CAR-modified EBV-CTLs persisted at a very low frequency *in vivo* (13). This limited engraftment may indicate that the endogenous presentation of latent EBV antigens, in the absence of virus reactivation, does not promote robust and durable engraftment of the infused CAR-redirected EBV-CTLs. In the allogeneic setting, we found enhanced engraftment of the infused CD19-specific CAR-redirected VsCTLs only in patients who were infused relatively early posttransplant, when higher EBV or CMV viral loads can fully stimulate the infused CAR-redirected VsCTLs through their native T-cell

[1]Center for Cell and Gene Therapy, Baylor College of Medicine, Houston Methodist Hospital and Texas Children's Hospital, Houston, Texas. [2]Department of Pediatrics, Baylor College of Medicine, Houston, Texas. [3]Department of Immunology, Baylor College of Medicine, Houston, Texas. [4]Department of Medicine, Baylor College of Medicine, Houston, Texas.

Note: Supplementary data for this article are available at Clinical Cancer Research Online (http://clincancerres.aacrjournals.org/).

Corresponding Author: Gianpietro Dotti, Center for Cell and Gene Therapy, Baylor College of Medicine, 6621 Fannin St/MC 3-3320, Houston, TX 77030. Phone: 832-824-6891; Fax: 832-825-4732; E-mail: gdotti@bcm.edu

doi: 10.1158/1078-0432.CCR-14-2998

Published OnlineFirst February 17, 2015; DOI: 10.1158/1078-0432.CCR-14-2998

Translational Relevance

T cells recognizing viral antigens such as Epstein–Barr virus (EBV) and cytomegalovirus (CMV) acquire tumor specificity when genetically modified to express a chimeric antigen receptor (CAR). Prolonged expansion and persistence of adoptively transferred tumor-specific T cells *in vivo* are a critical step in achieving sustained clinical responses. Here, we provide data showing that a K562-based whole-cell vaccine generated to express the viral antigen CMV-pp65 and immune stimulatory molecules CD40L and OX40L enhances the antitumor effects of CMV-cytotoxic T cells (CTL) expressing a CAR by boosting their intrinsic virus specificity.

receptors (12). In contrast, engraftment remains suboptimal if the cells are infused late after transplant when the probability of experiencing virus reactivations is rather low (12).

On the basis of the clinical evidence, we hypothesized that an intentional *in vivo* vaccine-mediated stimulation of adoptively transferred CAR-modified VsCTLs would produce enhanced engraftment and superior antitumor effect of these cells. We developed a whole-cell vaccine that promotes the cross-presentation of viral epitopes to the native virus-specific T-cell receptors of CAR-redirected VsCTLs. The proposed approach is preferable to a vaccine aimed at boosting CAR-redirected VsCTLs through their CAR specificity, since only APCs processing and presenting viral antigens in the MHC context can fully and physiologically induce T-cell costimulation.

A whole-cell vaccine approach based on the administration of irradiated allogeneic immortalized cell lines engineered to express immune-modulatory cytokines such as IL2 and GM-CSF to cross-present antigens to host APCs has been used in several clinical trials (14–18). On the basis of these clinical findings, we prepared a whole-cell vaccine by engineering the K562 cell line to stimulate, via antigen cross-presentation, the intrinsic virus-specificity of CAR-modified VsCTLs *in vivo*. As proof of principle, we selected to engineer the K562 cell line with the CMV-pp65 protein to stimulate CAR-redirected CMV-CTLs (CAR-CMV-CTLs) based on the high frequency of CMV seropositive individuals (19) and the robust evidence that $CD8^+$ T cells specific for the CMV-pp65 protein play a dominant protective role in CMV infections (20).

We envisioned further engineering K562 to express CD40L and OX40L immune stimulatory molecules to strengthen the effect of our vaccine. CD40L promotes the maturation of APCs and directly activates $CD8^+$ T cells (21–23), whereas OX40L promotes the recruitment of $CD4^+$ T cells (24–26), which play an important role in controlling tumor growth in clinical trials of adoptive T-cell transfer (13). We then conducted experiments to show that the K562-derived whole-cell vaccine can safely and effectively stimulate CAR-CMV-CTLs *in vitro* and *in vivo*, enhancing their overall antitumor activity.

Materials and Methods

Cell line

K562, Raji, and A459 tumor cells were purchased from ATCC. K562 and Raji cells were cultured in RPMI-1640 (HyClone, Thermo Scientific) supplemented with 10% FBS (HyClone) and 2 mmol/L GlutaMax (Invitrogen). A549 tumor cell line was cultured in DMEM (Gibco, Invitrogen) supplemented with 10% FBS and 2 mmol/L GlutaMax. A459 was single cell cloned based on the expression of the GD2 antigen. The neuroblastoma cell line CHLA-255 (ref. 27; kindly provided by Dr. Leonid Metelitsa, Baylor College of Medicine, Houston TX) was derived from a patient. CHLA-255 was cultured in IMDM (Gibco, Invitrogen) supplemented with 10% FBS and 2 mmol/L GlutaMax, and we verified that this line retains the surface expression of the target antigen GD2. Cells were maintained in a humidified atmosphere containing 5% CO_2 at 37°C. All cell lines were routinely tested to ensure that they were mycoplasma free and authenticated based on short tandem repeats (STR) at MD Anderson Cancer Center (Houston, TX) except for CHLA-255. For the coculture experiments, CHLA-255 and Raji cells were transduced with a retroviral vector encoding GFP (>98% GFP^+ cells).

Isolation of peripheral blood mononuclear cells and generation of dendritic cells

Peripheral blood mononuclear cells (PBMC) were isolated from buffy coats (Gulf Coast Regional Blood Center) or blood donations from healthy donors (under Institutional Review Board-approved protocol, BCM) using Ficoll–Paque (Amersham Biosciences). Monocytes were obtained from PBMCs by positive magnetic selection with CD14 magnetic beads (Miltenyi Biotec). Dendritic cells (DCs) were generated from $CD14^+$ cells cultured in DC media (CellGenix) supplemented with IL4 (1,000 U/mL) and GM-CSF (800 U/mL; R&D Systems). On day 5, DCs were matured with IL6 (1 μg/mL), TNFα (1 μg/mL), IL1β (1 μg/mL), and prostaglandin E (1 μg/mL; all from R&D Systems, Inc) for 48 hours.

K562-derived whole-cell vaccine

The vaccine was generated using the K562 cell line. These cells were transduced with lentiviral vectors encoding either human CD40L or OX40L or pp65/eGFP or the combination CD40L/pp65 or OX40L/pp65. After transduction, single cell clones were obtained. For selected experiments, K562 clones were also genetically modified with a retroviral vector to stably express the inducible caspase-9 suicide gene (*iC9*; ref. 28).

Generation of autologous phytohemagglutinine-activated T cells and lymphoblastoid cell lines

To generate PHA blasts, PBMCs were stimulated with the mitogen phytohemagglutinine-P (PHA-P, 5 μg/mL; Sigma-Aldrich). PHA blasts were then expanded in RPMI-1640 supplemented with 5% human serum (Valley Biomedical) and 2 mmol/L Glutamax, and in the presence of IL2 (100 U/mL; Teceleukin, Chiron Therapeutics). The lymphoblastoid cell lines (LCLs) were generated as previously described (29).

Activation of monocytes by K562-derived whole-cell vaccine

Monocytes were stained with the PKH26 red fluorescent cell linker compound and then cocultured at a ratio of 5:1 with irradiated K562 labeled with PKH2 green fluorescent cell linker compound (Sigma-Aldrich). After 72 hours, we analyzed the expression of activation/maturation markers in monocytes by flow cytometry, testing the level of expression of CD11c, CD80, CD83, and HLA-DR. Moreover, we monitored the coculture by a fluorescence microscope.

Published OnlineFirst February 17, 2015; DOI: 10.1158/1078-0432.CCR-14-2998

Generation of retroviral supernatant and transduction of VsCTLs

Retroviral supernatants were produced in 293T cells, as previously described (30). Lentivirus supernatants were produced in 293T cells cotransfected with the lentiviral vector and separated plasmids encoding the *VSV-G* envelope, *gag-pol*, and *REV* (31). To generate CMV-CTLs, PBMCs from CMV seropositive donors were stimulated with DCs (20:1) loaded with the CMV-pp65 pepmix (HCMVA, JPT) at 5 μmol/L for 2 hours at 37°C in 5% CO_2. Cells were then plated in complete media containing RPMI-1640 45%, Clicks medium (Irvine Scientific) 45%, 10% human AB serum, and 2 mmol/L GlutaMax. After 10 days, T cells were restimulated with DCs loaded with the same pepmix. After the second round of stimulation, cells were expanded and fed with IL2 (50 U/mL; Proleukin, Chiron). Three days later, cells were transduced with a retroviral vector encoding a CAR specific for the GD2 antigen and containing the CD28 endodomain (CAR-GD2) using retronectin-coated plates (Takara Bio Inc; ref. 12).

Stimulation of PBMCs and CMV-CTLs using K562-derived whole-cell vaccine

PBMCs from seropositive donors were incubated with irradiated K562 (80–100 Gy) at a ratio of 10:1 for 10 to 12 days in the absence of cytokines. Transduced CAR-CMV-CTLs were stimulated weekly with irradiated K562 and autologous CD3-depleted PBMCs at a ratio of 5:1:1 (CTLs:K562:PBMCs CD3-depleted) and fed with IL2 (50 U/mL) twice/week.

IFNγ Enzyme-Linked Immunospot Assay (ELISpot)

The IFNγ ELISpot assay was performed as previously described (8). T cells were plated in triplicate at 10^5 cells/well with 5 μmol/L of CMV-pp65 pepmix. In all experiments, T cells were also incubated with an irrelevant pepmix, as negative control, or stimulated with 25 ng/mL of phorbol myristate acetate (PMA; Sigma-Aldrich) and 1 μg/mL of ionomycin (Iono; Sigma-Aldrich) as positive control. In selected experiments, CAR-CMV-CTLs were tested in ELISpot plates coated with both IFNγ antibody and anti-idiotype antibody (1A7) that induces cross-link of CAR molecules (11).

Flow cytometry

For phenotypic analysis, we used CD11c, CD80, CD83, HLA-DR, CD45, CD56, CD19, CD8, CD4, and CD3 mAbs (all from Becton Dickinson) conjugated with FITC, PE, PerCP, or APC fluorochromes. The expression of CAR-GD2 was detected using the 1A7 Ab. Samples were analyzed with a BD FACScalibur system equipped with the filter set for quadruple fluorescence signals and the CellQuest software (BD Biosciences). For each sample, we analyzed a minimum of 30,000 events. CTLs were also analyzed for binding of specific tetramers. Tetramers were prepared by the Baylor College of Medicine (Houston, TX) core facility. For each sample, a minimum of 100,000 cells were analyzed.

Chromium-release assay

The cytotoxic activity of T cells was evaluated using a standard 4-hour ^{51}Cr-release assay, as previously described (9). Target cells were incubated in medium alone or in 1% Triton X-100 (Sigma-Aldrich) to determine spontaneous and maximum ^{51}Cr-release, respectively. The mean percentage of specific lysis of triplicate wells was calculated as follows: [(test counts − spontaneous counts)/(maximum counts − spontaneous counts)] × 100. The target cells tested included CHLA-255, Raji, and PHA blasts loaded with irrelevant or CMV-pp65 pepmixes.

Western blot analysis

Proteins were extracted from 5×10^6 cells, using RIPA lysing buffer (Cell Signaling Technology) supplemented with a protease inhibitor cocktail (Sigma-Aldrich). Of note, 50 μg of protein were resolved by SDS-PAGE, transferred to polyvinylidene difluoride membranes (Bio-Rad), and blocked with 5% (W/V) nonfat dry milk in TBS with 0.1% (V/V) Tween-20. Blots were stained with mouse anti-CMV-pp65 (1:200, clone 1-L-11; Santa Cruz Biotechnology) and mouse anti-human β-actin (1:10000, clone C4; Santa Cruz Biotechnology). Blots were washed with TBS containing 0.1% (V/V) Tween-20, stained with horseradish peroxidase-conjugated secondary Ab (1:5000, goat anti-mouse sc-2005; Santa Cruz Biotechnology), and incubated with SuperSignal West Femto Maximum Sensitivity Substrate (Thermo Scientific).

Xenogenic SCID mouse models

Mouse experiments were performed in accordance with Baylor College of Medicine's Animal Husbandry guidelines following Institutional Animal Care and Use Committee-approved protocols. In the first set of experiments, we tested the ability of the K562-derived whole-cell vaccine to stimulate CMV-CTLs from PBMCs collected from healthy CMV-seropositive donors. Figure 2A summarizes the design of the experiment. Eight- to 10-week-old NOG/SCID/$\gamma_c^{-/-}$ mice (Jackson Lab) received three inoculations intraperitoneally (i.p.) and intravenously (i.v.) of 5×10^6 PBMCs (32) and 10^6 irradiated K562 and were euthanized by day 14 for analysis of immune responses. For the antitumor effects, two models were tested. In the first model, NOG/SCID/$\gamma_c^{-/-}$ mice were implanted i.p. with CHLA-255 cells (2.5×10^6), labeled with firefly luciferase, and resuspended in Matrigel (Becton Dickinson Biosciences). Tumor growth was measured by *in vivo* bioluminescence using the Lumina IVIS *in vivo* imaging system (PerkinElmer; ref. 33). Five days after tumor inoculation, control and CAR-CMV-CTLs were injected i.p. (10×10^6 cells/mouse). Mice were subsequently vaccinated according to the schedule illustrated in Fig. 2A. IL2 (1,000 U/mouse) was also administered i.p. twice a week for 2 weeks. In the systemic tumor model, NOG/SCID/$\gamma_c^{-/-}$ mice were infused via tail injection with GD2$^+$ A459 tumor cells labeled with firefly luciferase (6×10^5 cells). On day 3, mice were injected i.v. with control or CAR-CMV-CTLs (8×10^6 cells/mouse) and vaccinated with K562 as described in Fig. 2A. Tumor growth was monitored by using the Lumina IVIS imaging system. Mice were euthanized when signs of discomfort were detected by the investigator or as recommended by the veterinarian who monitored the mice three times a week or when luciferase signal reached 7.5×10^7 p/sec/cm^2/sr. For the validation of the *iC9* suicide gene, mice were engrafted with K/CD40L/pp65 and K/OX40L/pp65 clones expressing *iC9* and an enhanced firefly luciferase gene (34). After engraftment, mice were infused intraperitoneally with the dimerizing drug AP20187 (50 μg/mouse; Clontech Lab) for 2 consecutive days. K562 growth was followed by *in vivo* bioluminescence.

Statistical analyses

Unless otherwise noted, data are summarized as mean ± SD. Student *t* test was used to determine statistically significant

Published OnlineFirst February 17, 2015; DOI: 10.1158/1078-0432.CCR-14-2998

differences between samples, with P value <0.05 indicating a significant difference. When multiple comparison analyses were required, statistical significance was evaluated by one-way ANOVA. Survival analysis was performed using the Kaplan–Meier method in GraphPad Software. The log-rank test was used to assess statistically significant differences between groups of mice. All P values <0.05 were considered statistically significant.

Results

K562-derived whole-cell vaccine encoding CMV-pp65 and CD40L stimulates CMV-CTLs *in vitro* by mediating antigen cross-presentation

To develop a whole-cell vaccine capable of boosting CMV-CTLs, we engineered the K562 cell line to express CMV-pp65, CD40L and OX40L molecules as follows: CD40L/pp65 (K/CD40L/pp65), OX40L/pp65 (K/OX40L/pp65), CD40L (K/CD40L), OX40L (K/OX40L), or pp65 (K/pp65). K/pp65 also expressed GFP, as a marker of selection. Single cell clones of engineered K562 were used for all the experiments. The expression of CD40L and OX40L was confirmed by FACS analysis (Fig. 1A), whereas the expression of pp65 was assessed by Western blot analysis (Fig. 1B). To ensure *in vitro* that engineered and irradiated K562 cells promote antigen cross-presentation, we proved that apoptotic bodies derived from irradiated K562 were uptaken by monocytes. As shown in Fig. 1C, freshly isolated monocytes (stained with red fluorescent) were cocultured for 3 days with either irradiated K/pp65 or K/CD40L/pp65 (stained with green fluorescent). Monocytes engulfed K562-derived apoptotic bodies (stained with yellow fluorescent) and expressed CD80 and CD83, and showed more pronounced upregulation of CD11c and HLA-DR only in the presence of CD40L (Fig. 1D). OX40L is not known to promote maturation of APCs, therefore it was unsurprising that the effects of K/OX40L/pp65 on the induction of CD80 and CD83 molecules on cultured monocytes were similar to those observed using K/pp65 (Supplementary Fig. S1).

The capacity of the whole-cell vaccine to stimulate *ex vivo* CMV-CTLs was assessed by coculturing PBMCs collected from CMV seropositive donors with engineered and irradiated K562 for 10 to 12 days. As positive controls, the same PBMCs were cultured in the presence of CMV-pp65 pepmix. After 10 to 12 days of culture, we found more $CD3^+CD8^+$ T cells in K/CD40L/pp65 and K/OX40L/pp65 (22% ± 5%) compared with K/pp65 (14% ± 4%; P = 0.002), and also more $CD3^+CD4^+$ T cells (42% ± 9% vs. 33% ± 11%; P = 0.002). The NK cells were 47% ± 15% in K/pp65 and 31% ± 14% in K/CD40L/pp65 and K/OX40L/pp65 (P = 0.014; Table 1). When assayed against CMV-pp65 pepmix, we found that K/pp65 effectively stimulated CMV-CTLs (292 ± 56 $IFN\gamma^+$ SFU/10^5 cells) and that the presence of CD40L (K/CD40L/pp65) further enhanced this effect (502 ± 104 $IFN\gamma^+$ SFU/10^5 cells; P = 0.034; Fig. 1E), although not as effectively as the positive control condition in which PBMCs were directly stimulated with CMV-pp65 pepmix (789 ± 130 $IFN\gamma^+$ SFU/10^5 cells). The presence of OX40L (K/OX40L/pp65) did not enhance the stimulatory effect observed with K/pp65 (357 ± 40 $IFN\gamma^+$ SFU/10^5 cells; P = ns). The combination of K/CD40L/pp65 and K/OX40L/pp65 did not further increase the frequency of CMV-CTLs (477 ± 91 $IFN\gamma^+$ SFU/10^5 cells; Fig. 1E). Pulsing T cells with an irrelevant pepmix produced negligible IFNγ reactivity (<30 $IFN\gamma^+$ SFU/10^5 cells; Fig. 1E). Overall, these data indicate that K/CD40L/pp65 can efficiently stimulate CMV-CTLs *in vitro* from PBMCs collected from seropositive donors.

CD40L and OX40L expressed by K562-derived whole-cell vaccine cooperate in stimulating CMV-CTLs *in vivo*

We assessed the capacity of the whole-cell vaccine to stimulate *in vivo* CMV-CTLs using NOG/SCID/$\gamma_c^{-/-}$ mice. Animals were coinfused with freshly isolated PBMCs obtained from CMV-seropositive donors and vaccinated twice with irradiated whole-cell vaccines and PBMCs as a source of APCs. CMV-specific immune responses were measured 7 days after the last vaccination (Fig. 2A). At the time of analysis, human $CD45^+$ cells engrafted in the spleen of mice from all groups, though engraftment was lower in mice vaccinated with K/pp65 as compared with mice vaccinated with K/CD40L/OX40L (P = 0.014) or K/CD40L/pp65 and K/OX40L/pp65 (P = 0.033; Fig. 2B). Although the immunophenotype of engrafted human $CD45^+$ cells isolated from the spleen showed a similar distribution in $CD3^+CD4^+$, $CD3^+CD8^+$, and NK cells (Fig. 2C), the antigen specificity of engrafted T cells was significantly different. As shown in Fig. 2D, in all experimental conditions T cells recovered from the spleen of mice vaccinated had detectable CMV-specific IFNγ production. However, the vaccination with combined K/CD40L/pp65 and K/OX40L/pp65 stimulated the highest CMV-specific response (101 ± 21 $IFN\gamma^+$ SFU/10^5 cells) compared with controls K/CD40L/OX40L (28 ± 6 $IFN\gamma^+$ SFU/10^5 cells; P < 0.001), K/pp65 (53 ± 22 $IFN\gamma^+$ SFU/10^5 cells; P = 0.048) and K/CD40L/pp65 (41 ± 14 $IFN\gamma^+$ SFU/10^5 cells; P = 0.033). In contrast with the *in vitro* experiments, *in vivo* data supported a critical role for the combination of CD40L- and OX40L-mediated activation in stimulating CMV-CTLs.

Virus specificity of "dual-specific" CAR-CMV-CTLs is boosted *in vitro* by the K562-derived whole-cell vaccine

To assess whether the whole-cell vaccines can be used to boost "dual-specific" CAR-CMV-CTLs, we generated CMV-CTLs as previously described (10, 12) and engrafted them with the CAR-GD2. The transduction efficiency of CMV-CTLs exposed to the retroviral supernatant encoding the CAR-GD2 ranged between 35% and 65%, as detected by flow cytometry. CAR-CMV-CTLs were then stimulated twice, one week apart, with engineered and irradiated K562 and autologous PBMCs (as a source of APCs), and assessed for phenotype and IFNγ production by ELISpot. CAR-CMV-CTLs stimulated with combined K/CD40L/pp65 and K/OX40L/pp65 showed a significant enrichment in specific precursors responding to the CMV-pp65 pepmix as assessed by IFNγ ELISpot assay (1,397 ± 212 $IFN\gamma^+$ SFU/10^5 cells) compared with CTLs stimulated with control K/CD40L/OX40L (749 ± 146 $IFN\gamma^+$ SFU/10^5 cells; P < 0.001; Fig. 3A). Similarly, CAR-restricted responses, measured after stimulation with the anti-idiotype 1A7 Ab that cross-links CAR-GD2 molecules, significantly increased in CAR-CMV-CTLs stimulated with K/CD40L/pp65 and K/OX40L/pp65 (2,819 ± 452 $IFN\gamma^+$ SFU/10^5 cells) compared with CTLs stimulated with control K/CD40L/OX40L (1,610 ± 267 $IFN\gamma^+$ SFU/10^5 cells; P = 0.009; Fig. 3A). In HLA-$A2^+$ donors, phenotypic analysis confirmed a significant enrichment in NLV-$tetramer^+$ and CAR^+ CTLs after stimulations with K/CD40L/pp65 and K/OX40L/pp65 (Fig. 3B).

We explored the retained effector function of CAR-CMV-CTLs stimulated *in vitro* with K/CD40L/pp65 and K/OX40L/pp65 against CMV-$pp65^+$ target and neuroblastoma $GD2^+$ cells

Published OnlineFirst February 17, 2015; DOI: 10.1158/1078-0432.CCR-14-2998

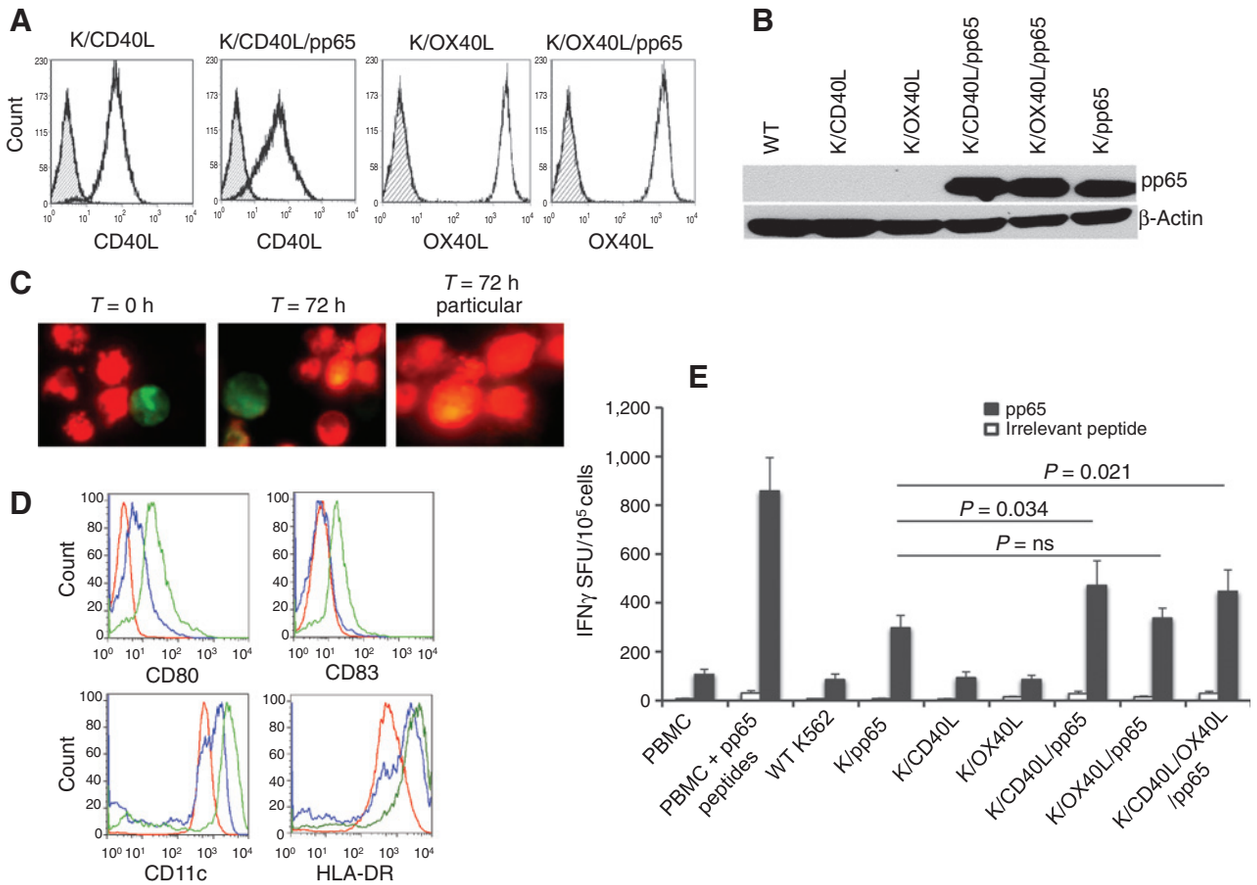

Figure 1.
K562-based whole-cell vaccine encoding CMV-pp65 and CD40L matures monocytes and stimulates CMV-CTLs *in vitro*. A, expression of CD40L and OX40L in engineered K562. Striped histograms indicate wild-type K562 cells. B, Western blot analysis showing the expression of CMV-pp65 in engineered K562. C, uptake of apoptotic bodies from irradiated K/pp65 and K/CD40L/pp65 by monocytes. Monocytes labeled with PKH26 red fluorescent cell linker compound were cocultured (5:1 ratio) with irradiated K/CD40L/pp65 labeled with PKH2 green fluorescent cell linker compound. Analysis of fluorescence signals was performed after 72 hours of coculture using a fluorescence microscope (Olympus IX70). D, expression of CD80, CD83, CD11c and HLA-DR by monocytes 72 hours after coculture with irradiated K/pp65 (in blue) and K/CD40L/pp65 (in green). The red line represents the expression of CD80, CD83, CD11c, and HLA-DR before the stimulation. E, frequency of CMV-CTLs assessed by IFNγ ELISpot using the CMV-pp65 pepmix. Data represented mean ± SD of 11 CMV-seropositive donors. Stimulation with an irrelevant pepmix was used as a negative control.

through their native TCRs and CAR, respectively. In a standard ^{51}Cr-release assay, CAR-CMV-CTLs showed cytotoxic activity against the GD2$^+$ target (CHLA-255; 63% ± 14%) and pp65-pepmix loaded PHA blasts (59% ± 3%; at 20:1 E:T ratio), but not against the GD2$^-$ target cell line (Raji) or PHA blasts loaded with an irrelevant pepmix (Fig. 3C and Supplementary Fig. S1). Control CMV-CTLs not expressing the CAR showed no activity against CHLA-255 (data not shown). Similar results were obtained by measuring IFNγ production in ELISpot assays. We plated CTLs and tumor cells at a ratio of 1:1, and after 24 hours, CAR-CMV-CTLs stimulated with K/CD40L/pp65 and K/OX40L/pp65 in response to CHLA-255 showed a trend for a higher IFNγ production (421 ± 21 IFNγ$^+$ SFU/10^5 cells) as compared with CAR-CMV-CTLs stimulated with K/CD40L/OX40L (295 ± 81 IFNγ$^+$ SFU/10^5 cells; $P = 0.6$; Fig. 3D). Reactivity against Raji cells (GD2$^-$ targets) was low in all experimental conditions. In coculture experiments in which CTLs and tumor cells were plated at a 1:1 ratio and cultured for 4 days, CAR-CMV-CTLs retained their capacity to eliminate CHLA-255 but not Raji (Fig. 3E). Overall, these data indicate that CAR-CMV-CTLs stimulated with K/CD40L/pp65 and K/OX40L/pp65 retain their selective specificities for CMV-pp65 and GD2 antigens.

Table 1. Phenotype of T cells collected by day 10 to 12 after coculture with K562-based whole-cell vaccine

	CD3$^+$/CD4$^+$	CD3$^+$/CD8$^+$	CD3$^-$/56$^+$
PBMC/pp65 pepmix	48% ± 27%	45% ± 29%	5% ± 2%
K562 wild-type	46% ± 11%	17% ± 2%	29% ± 10%
K/pp65	33% ± 11%	14% ± 4%	47% ± 15%
K/CD40L	42% ± 7%	23% ± 7%	30% ± 5%
K/OX40L	40% ± 5%	20% ± 6%	33% ± 6%
K/CD40L/pp65	43% ± 11%	22% ± 3%	31% ± 13%
K/CD40L/pp65 + K/OX40L/pp65	42% ± 9%	22% ± 5%	31% ± 14%

Vaccination with K562-derived whole-cell vaccine encoding CMV-pp65, CD40L, and OX40L increases the antitumor effect of "dual specific" CAR-CMV-CTLs

To assess whether vaccination with the K562-derived whole-cell vaccine increases the antitumor effects of CAR-CMV-CTLs,

Published OnlineFirst February 17, 2015; DOI: 10.1158/1078-0432.CCR-14-2998

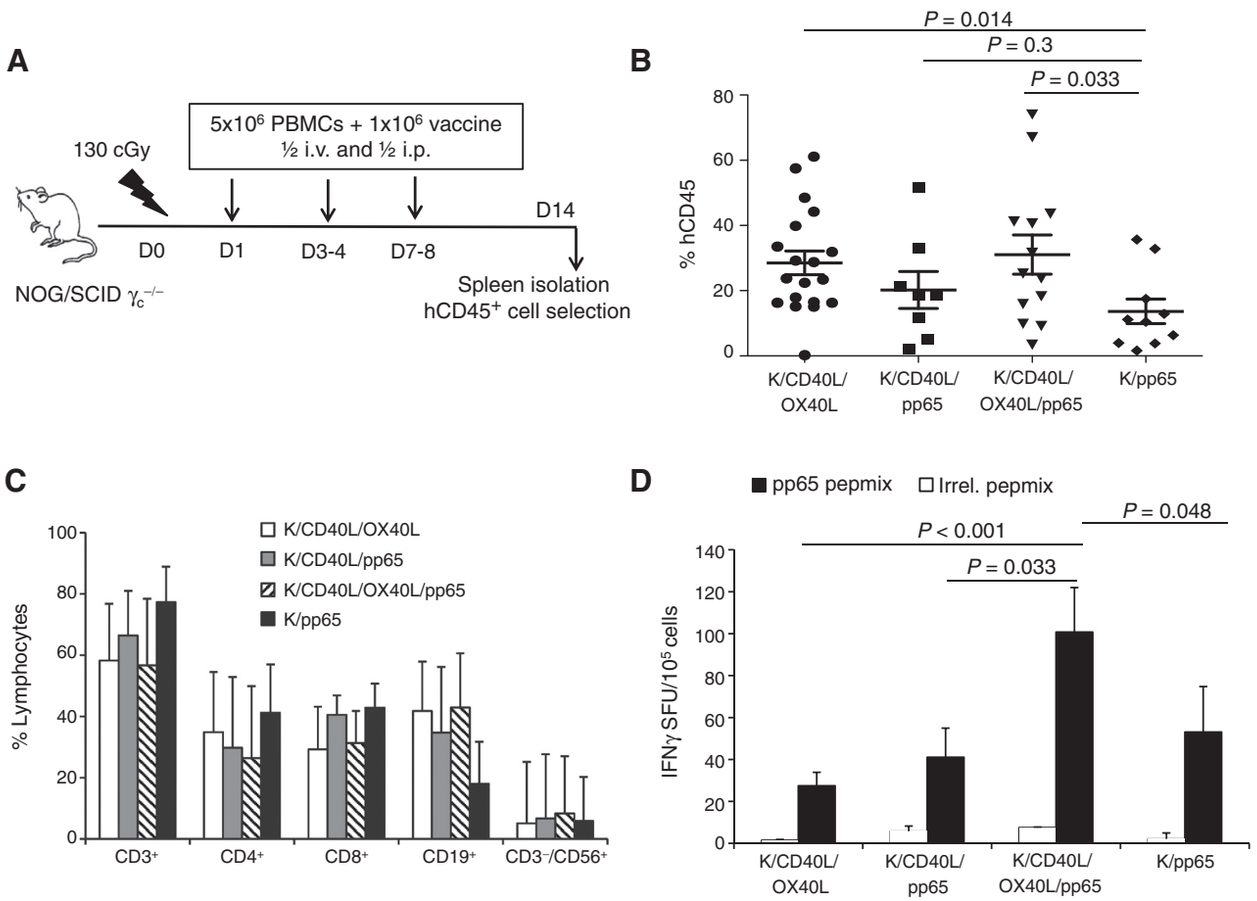

Figure 2.

Coexpression of CD40L and OX40L by K562-derived whole-cell vaccine maximizes the stimulation of CMV-CTLs *in vivo*. A, schematic representation of the xenograft mouse model in NOG/SCID/$\gamma_c^{-/-}$ mice. B, engraftment of human CD45$^+$ cells in the spleen, 14 days after vaccination. C, phenotypic analysis of human CD45$^+$ cells engrafted in the spleen by day 14. Data represent mean ± SD of 8 mice per group. D, enumeration of the CMV-CTLs in isolated human CD45$^+$ cells as assessed by IFNγ ELISpot in response to CMV-pp65 and irrelevant pepmixes. Data represent mean ± SD of 8 mice per group.

NOG/SCID/$\gamma_c^{-/-}$ mice were implanted intraperitoneally with CHLA-255 cells labeled with firefly luciferase. Five days after tumor implant, mice received intraperitoneal control or CAR-CMV-CTLs followed by the vaccination schedule illustrated in Fig. 2A. Mice vaccinated with the K/CD40L/pp65 and K/OX40L/pp65 combination controlled tumor growth significantly better by day 50 than mice vaccinated with K/CD40L/OX40L ($P = 0.011$; Fig. 4A). Tumor control was CAR mediated, since tumors grew despite vaccinations with K/CD40L/pp65 and K/OX40L/pp65 in mice infused with control CMV-CTLs (Fig. 4A). We selected day 50 to stop the experiment and to assess macroscopically for the presence of tumor at the time of euthanasia. We found that although only 2 out of 17 (12%) mice vaccinated with K/CD40L/OX40L were tumor free, 8 out of 17 (47%) mice were tumor free in the group vaccinated with K/CD40L/pp65 and K/OX40L/pp65. In addition, tumors were significantly smaller in mice vaccinated with K/CD40L/pp65 and K/OX40L/pp65 compared with mice receiving control CMV-CTLs ($P < 0.0001$) or CAR-CMV-CTLs and control K/CD40L/OX40L vaccine ($P = 0.022$; Fig. 4B). Human CD45$^+$ T cells recovered from the spleen of mice vaccinated with combined K/CD40L/pp65 and K/OX40L/pp65 also showed the highest frequency of CMV-CTLs (85 ± 16 IFNγ$^+$ SFU/10^5 cells) compared with mice vaccinated with the control K/CD40L/OX40L (41 ± 11 IFNγ$^+$ SFU/10^5 cells; $P = 0.035$). We measured CAR-dependent immune responses after stimulation with the anti-idiotype 1A7 Ab. Similar to above, responses were increased in T cells recovered from the spleen of mice vaccinated with combined K/CD40L/pp65 and K/OX40L/pp65 (71 ± 24 IFNγ$^+$ SFU/10^5 cells) compared with mice vaccinated with control K/CD40L/OX40L (23 ± 8 IFNγ$^+$ SFU/10^5 cells; $P = 0.048$; Fig. 4C).

We further validated the vaccination approach in a systemic model. For these experiments, NOG/SCID/$\gamma_c^{-/-}$ mice were infused intravenously with a single cell derived clone of the A459 tumor cell line that expresses GD2 and rapidly metastasizes upon lung engraftment. Tumor cells were labeled with firefly luciferase to measure tumor bioluminescence *in vivo*. In this model, control and CAR-CMV-CTLs were infused intravenously and the vaccination was performed as described in Fig. 2A. As illustrated in Fig. 4D, in this systemic model, vaccination with combined K/CD40L/pp65 and K/OX40L/pp65 also induced better control of tumor growth by CAR-CMV-CTLs, which translated into significantly improved overall survival ($P = 0.016$; Fig. 4E). Altogether, these data indicate that vaccination with combined

Published OnlineFirst February 17, 2015; DOI: 10.1158/1078-0432.CCR-14-2998

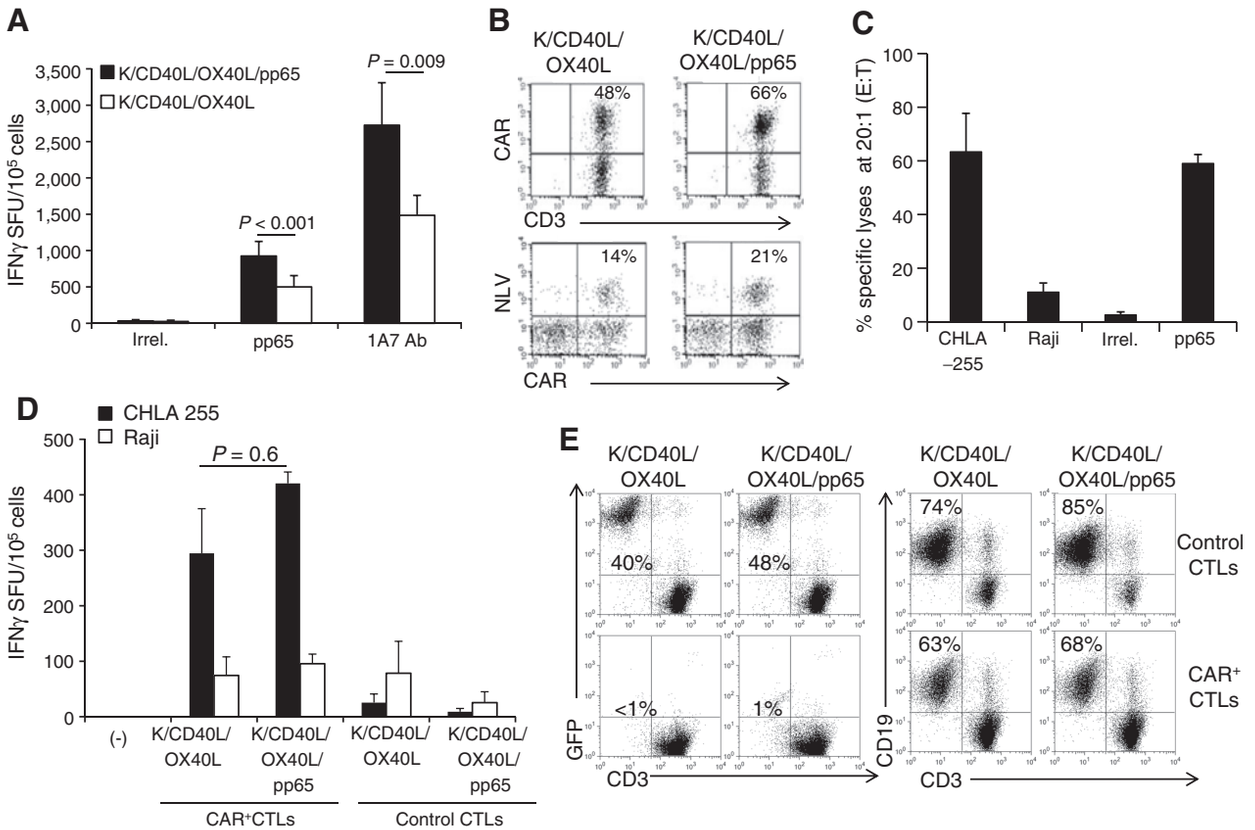

Figure 3.

Virus specificity of "dual specific" CAR-CMV-CTLs is stimulated by K562-derived whole-cell vaccine *in vitro*. In these experiments, we compared the effector function of CAR-CMV-CTLs stimulated *in vitro* with control K/CD40L plus K/OX40L and K/CD40L/pp65 plus K/OX40L/pp65. A, enumeration of IFNγ-producing cells by ELISpot in response to the CMV-pp65 pepmix or the 1A7 Ab that cross-links the CAR-GD2. Data summarize mean ± SD of 9 donors. B, detection of CAR and NLV-tetramer in CAR-CMV-CTLs by flow cytometry in a representative HLA-A2$^+$ donor. Although the CAR staining detects all CAR-CMV-CTLs, the tetramer only identifies CAR-CMV-CTLs specific for one single epitope (NLV) in the context of one haplotype (HLA-A2.01). C, cytotoxic activity (^{51}Cr-release assay at a 20:1 effector:target ratio) against CHLA-255 neuroblastoma cells (GD2$^+$ cells) and Raji lymphoma cells (GD2$^-$ cells). PHA blasts pulsed with CMV-pp65 or irrelevant pepmixes were also used as target cells. Data summarize mean ± SD of 4 donors. D, frequency of IFNγ-producing cells in response to CHLA-255 and Raji at 1:1 effector:target ratio. Data summarize mean ± SD of 3 donors. E, antitumor activity of CAR-CMV-CTLs in coculture experiments against CHLA-255 (GD2$^+$ cells; right) and Raji cells (GD2$^-$ cells; left). Both CHLA-255 and Raji cells were transduced with a retroviral vector encoding GFP. Tumor cells and CAR-CMV-CTLs were plated at 1:1 ratios, and CAR-CMV-CTLs (CD3$^+$ cells) and tumor cells (GFP$^+$ cells) were quantified by flow cytometry after 4 days of coculture. Representative of 4 different donors.

K562-derived whole-cell vaccine K/CD40L/pp65 and K/OX40L/pp65 improves the antitumor effects of CAR-CMV-CTLs in xenograft models.

Activation of the *iC9* suicide gene expressed by the K562-derived whole-cell vaccine abrogates their tumorigenicity

For a potential clinical application, we sought to ensure the safety of this approach *in vivo* as the whole-cell vaccine is derived from a tumor cell line. For these experiments, K/CD40L/pp65 and K/OX40L/pp65 were labeled with an enhanced firefly luciferase that allows visualizing fewer than 10 cells in a mouse (35). Irradiation of K/CD40L/pp65 and K/OX40L/pp65 before inoculation into NOG/SCID/$\gamma_c^{-/-}$ mice completely abrogated the cells' tumorigenicity. As shown in Fig. 5C, when K/CD40L/pp65 and K/OX40L/pp65 were irradiated at 80 to 100 Gy before infusion, tumor growth was completely prevented in mice observed for more than 90 days. As an extra precaution, and to guarantee the safety of the vaccination, we further engineered the K562 cell line with the inducible suicide *iC9* that also expresses a truncated form of CD19 as a selectable marker (27). Single cell clones were selected based on the expression of CD19 (Fig. 5A and B). Cells were inoculated subcutaneously without irradiation (4×10^6 cells) into NOG/SCID/$\gamma_c^{-/-}$ mice. By day 15 after engraftment, mice received intraperitoneal AP20187 (50 μg/mouse) for 2 consecutive days. Mice monitored for more than 90 days did not develop the tumor (Fig. 5D–F). Overall, these data indicate that the safety of the vaccination with K/CD40L/pp65 and K/OX40L/pp65 can be further assured through the incorporation of the *iC9* suicide gene.

Discussion

We previously reported that the infusion of EBV-CTLs and CMV-CTLs expressing a CAR promotes objective tumor regressions in clinical trials (11–13). However, *in vivo* expansion and persistence of these cells remain suboptimal likely because, in the absence of significant amounts of viral load, the costimulation provided by endogenous APCs processing and presenting latent

Published OnlineFirst February 17, 2015; DOI: 10.1158/1078-0432.CCR-14-2998

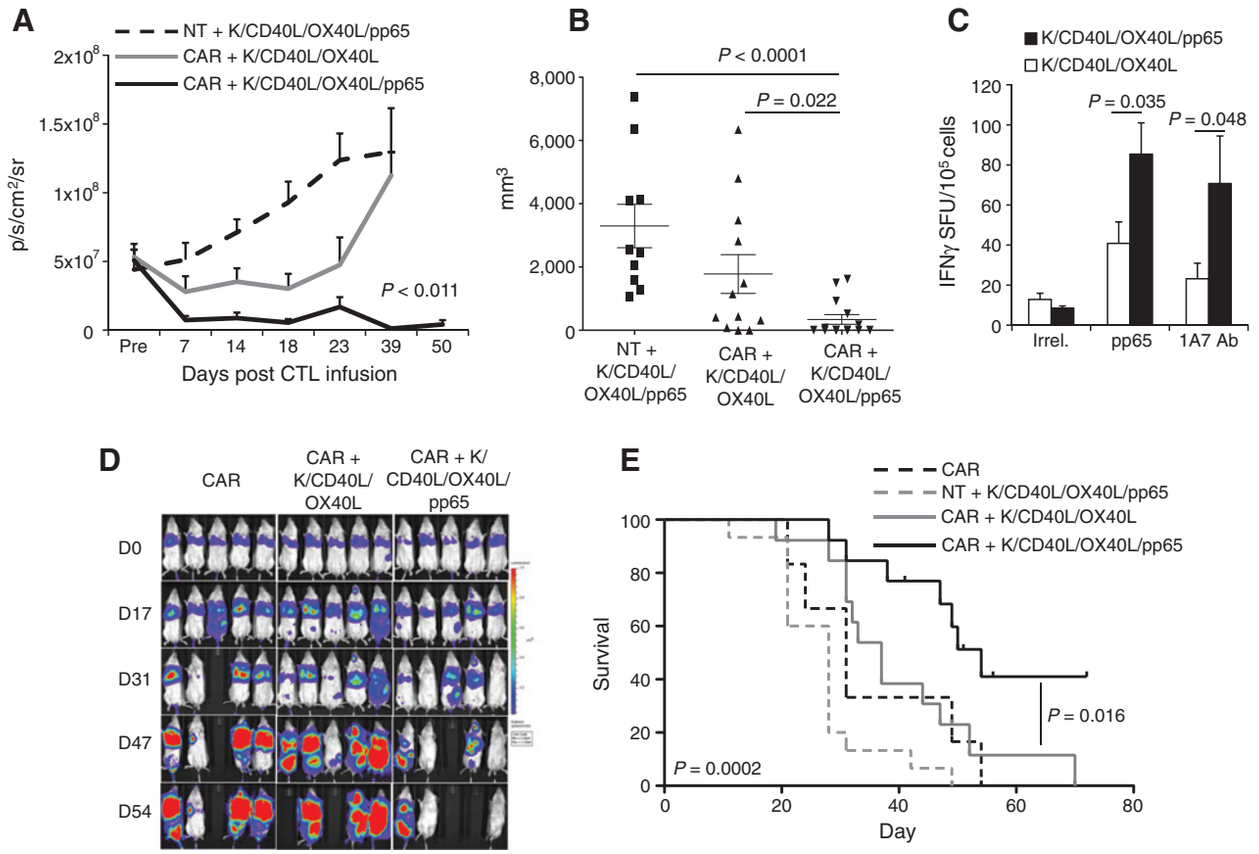

Figure 4.

Vaccination with K562-derived whole-cell vaccine expressing CMV-pp65, CD40L, and OX40L enhances antitumor effects of CAR-CMV-CTLs *in vivo*. A, NOG/SCID/$\gamma_c^{-/-}$ mice engrafted i.p. with the neuroblastoma cell line CHLA-255 labeled with firefly luciferase were infused i.p. with control or CAR-CMV-CTLs and vaccinated. The graph summarizes tumor bioluminescence. Summary of CMV-CTL lines prepared from 4 donors: 15 mice (control CMV-CTLs plus K/CD40L/pp65 and K/OX40L/pp65), 17 mice (CAR-CMV-CTLs plus K/CD40L and K/OX40L), and 17 mice (CAR-CMV-CTLs plus K/CD40L/pp65 and K/OX40L/pp65) were used per group. B, mice euthanized were analyzed for the presence of macroscopic tumors. The graph summarizes the volume of the tumor collected in the different groups. C, enumeration of the CMV-CTLs in the isolated human $CD45^+$ cells from the spleen as assessed by IFNγ ELISpot in response to CMV-pp65 and irrelevant pepmixes or the 1A7 Ab that cross-links the CAR-GD2. Data represent mean ± SD. D, mice were inoculated intravenously with the $GD2^+$ lung carcinoma cell line A459 labeled with firefly luciferase. Mice were then infused intravenously with control or CAR-CMV-CTLs and vaccinated. Tumor bioluminescence was then measured over time. The graph is representative of one of four experiments using CMV-CTLs from 4 donors. E, Kaplan–Meier analysis of tumor-bearing mice. Summary of CMV-CTL lines prepared from 4 donors: 15 mice (control CMV-CTLs plus K/CD40L/pp65 and K/OX40L/pp65), 13 mice (CAR-CMV-CTLs plus K/CD40L and K/OX40L), 13 mice (CAR-CMV-CTLs plus K/CD40L/pp65 and K/OX40L/pp65), and 8 mice (CAR-CMV-CTLs alone) were used per group.

viral antigens is insufficient to promote robust engraftment of CAR-redirected VsCTLs once infused. Here, we developed a strategy that can achieve the necessary engraftment. We have generated a vaccination approach using a K562-derived whole-cell vaccine and demonstrated that the antitumor effect of adoptively transferred CAR-redirect CMV-CTLs is enhanced when these CTLs are boosted *in vivo* by the vaccine.

Vaccination is the most common modality to induce both humoral and cellular immune responses. In the absence of clinically approved vaccines to induce cellular immune responses to either EBV or CMV, several experimental vaccination approaches for a clinical translation can be envisioned. These include DNA-plasmids (36), peptides (37), and *ex vivo* expanded and antigen-loaded DCs (38). However, each of these approaches has limitations that are primarily due to low immunogenicity (DNA-plasmid vaccine; ref. 39), toxicity caused by the strong adjuvants included in the vaccine preparation (peptide vaccine; ref. 40), and significant variability of the biologic characteristics of the final product and manufacturing costs (DC-based vaccine). On the basis of these limitations, we elected to generate an off-the-shelf whole-cell vaccine to boost *in vivo* adoptively transferred CAR-CMV-CTLs.

Autologous and allogeneic whole-cell vaccines consisting of tumor cells genetically manipulated to express GM-CSF or other cytokines, chemokines and immune stimulatory molecules have been used in clinical trials to promote cross-presentation of tumor-associated antigen to APCs *in vivo* (14, 15, 17, 41–43). On the basis of this evidence, we proposed to engineer the very well-characterized tumor cell line K562 to express the highly immunogenic CMV-pp65 protein. We thus created a whole-cell vaccine to administer to patients infused with CMV-CTLs expressing a tumor-specific CAR.

Our data demonstrate that the ectopic expression of the viral protein pp65 by K562 can be efficiently used to transfer the protein, likely in the form of apoptotic bodies, to APCs that can then process and present pp65 epitopes in the context of the

Published OnlineFirst February 17, 2015; DOI: 10.1158/1078-0432.CCR-14-2998

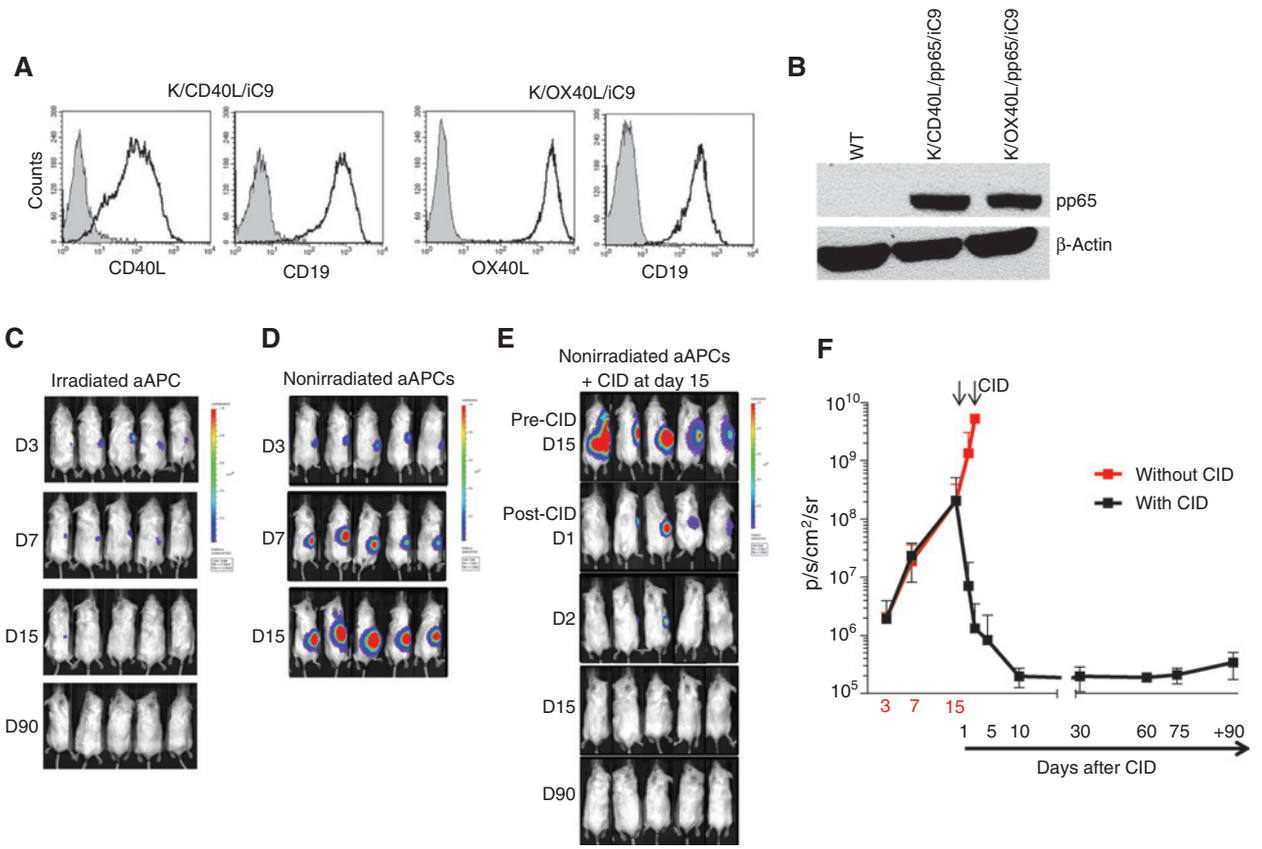

Figure 5.
Activation of the *iC9* suicide gene eliminates engrafted K562-derived whole-cell vaccine *in vivo*. A, characterization of the clones by flow-cytometric analysis. Gray areas indicate wild-type K562 cells. B, Western blot analysis showing the expression of CMV-pp65 in the clones expressing the *iC9* transgene. C and D, NOG/SCID/$\gamma_c^{-/-}$ mice were inoculated subcutaneously with irradiated (C) or nonirradiated (D) K562-derived whole-cell vaccine expressing the *iC9* gene and labeled with an enhanced firefly luciferase. Tumor growth was measured by *in vivo* imaging. E–F, effects of the administration of the chemical inducer of dimerization (CID) AP20187 on the growth of engineered vaccine. Arrows indicate the time of the CID administration.

appropriate MHC molecules. This approach, when applied directly *in vivo* to boost adoptively transferred CAR-CMV-CTLs, has the advantage of delivering preformed antigens to APCs without the need for the *in vivo* protein synthesis required by DNA-plasmid vaccines. In addition, such a cell-based vaccine easily can be further engineered to express other molecules to enhance immune responses. In our specific case, we selected CD40L and OX40L. We and others have used CD40L expression in the past to generate autologous vaccines for hematologic malignancies to induce the upregulation of the costimulatory molecules CD80 and CD86 in leukemic cells through the CD40-CD40L pathway (43–45). Here, we demonstrated that CD40L expressed in the whole-cell vaccine is essential in promoting the expression of CD80 and CD83 in monocytes engulfing apoptotic bodies. Control vaccine producing pp65 but lacking CD40L is indeed less efficient in that regard. Because CD80 and CD83 are upregulated in mature DCs to initiate immune responses (23, 46), CD40L expressed by the whole-cell vaccine seems to accomplish the crucial step of APC maturation upon antigen processing.

We also included OX40L in the K562-derived whole-cell vaccine. As illustrated by our data, OX40L does not play a role in inducing the expression of CD80 and CD83 by monocytes engulfing apoptotic bodies. As a consequence, K/OX40L/pp65 is not superior to control K/pp65 in boosting CMV-CTLs. We have previously combined CD40L and OX40L molecules/signaling showing that they mediate enhanced potency of an autologous leukemia vaccine (47). Consistent with that experience, we did not show an advantage in combining both CD40L and OX40L in short-term experiments *in vitro*, because OX40L mostly delivers critical late accessory signals that augment the proliferation and survival of memory $CD4^+$ T cells (48, 49). However, the combination CD40L and OX40L within the whole-cell vaccine showed clear benefits in *in vivo* experiments. We found in mice a more profound increase of CMV-CTLs when both CD40L and OX40L were incorporated within the whole-cell vaccine, suggesting the critical role of CD4 in boosting CMV-CTL responses. As a consequence, when CMV-CTLs are expressing a CAR, boosting *in vivo* their native virus specificity with the combination K/CD40L/pp65 and K/OX40L/pp65 showed better antitumor effects in two models of xenogenic solid tumors. Because K562 is also known to stimulate the proliferation of natural killer cells (NKs), we found *in vitro* and *in vivo* that the boosting with K562-derived whole-cell vaccine induced the expansion of NKs in addition to CAR-CMV-CTLs. Although no description of increased NKs has been

Published OnlineFirst February 17, 2015; DOI: 10.1158/1078-0432.CCR-14-2998

reported using K562/GM-CSF cells in patients (17), considering the antitumor effects of NKs, the *in vivo* boosting of this cell subset by the K562-derived whole-cell vaccine may be beneficial.

Finally, we also addressed the potential safety concerns raised by using tumor cells as a vaccine. Autologous and allogeneic tumor cell lines have been safely used in multiple large clinical trials, suggesting that irradiation before inoculation abrogates their growth. Despite this apparent safety, however, a lethal acute respiratory distress syndrome and severe eosinophilia were reported in a patient vaccinated with irradiated autologous myeloblasts admixed with GM-CSF secreting K562 (http://oba.od.nih.gov/oba/RAC/meetings/Dec2011/RAC_Minutes_12-11.pdf). We found in animals that irradiation abolishes the growth of our K562 engineered with pp65, CD40L, and OX40L. However, we also demonstrated that an additional safety mechanism can be implemented by further engineering these cells to express the *iC9* suicide gene. Activation of *iC9* by a small molecule halts the growth of live (deliberately nonirradiated) engineered K562 implanted in mice and since *iC9* has been validated in a clinical trial, it can be used efficiently in the context of a vaccine approach (27).

In conclusion, we demonstrated that a K562-derived whole-cell vaccine can safely enhance the antitumor effects of adoptively transferred CAR-CMV-CTLs. Due to the high flexibility of the whole-cell vaccine, K562 can be properly engineered to express other immunogenic antigens derived from other viruses and provide other relevant molecules to activate the immune system.

Disclosure of Potential Conflicts of Interest

B. Savoldo and G. Dotti are investigators in a collaborative research grant between the Center for Cell and Gene Therapy and Celgene to develop genetically modified T cells. No potential conflicts of interest were disclosed by the other authors.

Authors' Contributions

Conception and design: B. Savoldo, G. Dotti
Development of methodology: I. Caruana, B. Savoldo, G. Dotti
Acquisition of data (provided animals, acquired and managed patients, provided facilities, etc.): I. Caruana, G. Weber, B. Savoldo, G. Dotti
Analysis and interpretation of data (e.g., statistical analysis, biostatistics, computational analysis): I. Caruana, G. Weber, B. Savoldo, G. Dotti
Writing, review, and/or revision of the manuscript: I. Caruana, G. Weber, B. Savoldo, G. Dotti
Administrative, technical, or material support (i.e., reporting or organizing data, constructing databases): I. Caruana, B.C. Ballard, M.S. Wood
Study supervision: I. Caruana, G. Dotti

Acknowledgments

The authors thank Dr. Brian Rabinovich from the MD Anderson Cancer Center (Houston, TX) for providing the enhanced firefly luciferase gene and Catherine Gillespie from the Center for Cell and Gene Therapy for editing the article.

Grant Support

This work was supported in part by R01 CA142636 NIH-NCI, W81XWH-10-10425 Department of Defense, Technology/Therapeutic Development Award.

The costs of publication of this article were defrayed in part by the payment of page charges. This article must therefore be hereby marked *advertisement* in accordance with 18 U.S.C. Section 1734 solely to indicate this fact.

Received November 20, 2014; revised January 20, 2015; accepted February 9, 2015; published OnlineFirst February 17, 2015.

References

1. Eshhar Z, Waks T, Gross G, Schindler DG. Specific activation and targeting of cytotoxic lymphocytes through chimeric single chains consisting of antibody-binding domains and the gamma or zeta subunits of the immunoglobulin and T-cell receptors. Proc Natl Acad Sci U S A 1993;90:720–4.
2. Dotti G, Gottschalk S, Savoldo B, Brenner MK. Design and development of therapies using chimeric antigen receptor-expressing T cells. Immunol Rev 2014;257:107–26.
3. Kalos M, Levine BL, Porter DL, Katz S, Grupp SA, Bagg A, et al. T cells with chimeric antigen receptors have potent antitumor effects and can establish memory in patients with advanced leukemia. Sci Transl Med 2011;3:95ra73.
4. Maude SL, Frey N, Shaw PA, Aplenc R, Barrett DM, Bunin NJ, et al. Chimeric antigen receptor T cells for sustained remissions in leukemia. N Engl J Med 2014;371:1507–17.
5. Davila ML, Riviere I, Wang X, Bartido S, Park J, Curran K, et al. Efficacy and toxicity management of 19-28z CAR T cell therapy in B cell acute lymphoblastic leukemia. Sci Transl Med 2014;6:224ra25.
6. Savoldo B, Ramos CA, Liu E, Mims MP, Keating MJ, Carrum G, et al. CD28 costimulation improves expansion and persistence of chimeric antigen receptor-modified T cells in lymphoma patients. J Clin Invest 2011;121:1822–6.
7. Schwartz RH. Costimulation of T lymphocytes: the role of CD28, CTLA-4, and B7/BB1 in interleukin-2 production and immunotherapy. Cell 1992;71:1065–8.
8. Rossig C, Bollard CM, Nuchtern JG, Rooney CM, Brenner MK. Epstein–Barr virus-specific human T lymphocytes expressing antitumor chimeric T-cell receptors: potential for improved immunotherapy. Blood 2002;99:2009–16.
9. Savoldo B, Rooney CM, Di Stasi A, Abken H, Hombach A, Foster AE, et al. Epstein Barr virus specific cytotoxic T lymphocytes expressing the anti-CD30{zeta} artificial chimeric T-cell receptor for immunotherapy of Hodgkin disease. Blood 2007;110:2620–30.
10. Micklethwaite KP, Savoldo B, Hanley PJ, Leen AM, mmler-Harrison GJ, Cooper LJ, et al. Derivation of human T lymphocytes from cord blood and peripheral blood with antiviral and antileukemic specificity from a single culture as protection against infection and relapse after stem cell transplantation. Blood 2010;115:2695–703.
11. Pule MA, Savoldo B, Myers GD, Rossig C, Russell HV, Dotti G, et al. Virus-specific T cells engineered to coexpress tumor-specific receptors: persistence and antitumor activity in individuals with neuroblastoma. Nat Med 2008;14:1264–70.
12. Cruz CR, Micklethwaite KP, Savoldo B, Ramos CA, Lam S, Ku S, et al. Infusion of donor-derived CD19-redirected virus-specific T cells for B-cell malignancies relapsed after allogeneic stem cell transplant: a phase 1 study. Blood 2013;122:2965–73.
13. Louis CU, Savoldo B, Dotti G, Pule M, Yvon E, Myers GD, et al. Antitumor activity and long-term fate of chimeric antigen receptor-positive T cells in patients with neuroblastoma. Blood 2011;118:6050–6.
14. Borrello I, Pardoll D. GM-CSF-based cellular vaccines: a review of the clinical experience. Cytokine Growth Factor Rev 2002;13:185–93.
15. Nemunaitis J, Jahan T, Ross H, Sterman D, Richards D, Fox B, et al. Phase 1/2 trial of autologous tumor mixed with an allogeneic GVAX vaccine in advanced-stage non-small-cell lung cancer. Cancer Gene Ther 2006;13:555–62.
16. Rousseau RF, Haight AE, Hirschmann-Jax C, Yvon ES, Rill DR, Mei Z, et al. Local and systemic effects of an allogeneic tumor cell vaccine combining transgenic human lymphotactin with interleukin-2 in patients with advanced or refractory neuroblastoma. Blood 2003;101:1718–26.
17. Smith BD, Kasamon YL, Kowalski J, Gocke C, Murphy K, Miller CB, et al. K562/GM-CSF immunotherapy reduces tumor burden in chronic myeloid leukemia patients with residual disease on imatinib mesylate. Clin Cancer Res 2010;16:338–47.
18. Le DT, Pardoll DM, Jaffee EM. Cellular vaccine approaches. Cancer J 2010;16:304–10.

19. Staras SA, Dollard SC, Radford KW, Flanders WD, Pass RF, Cannon MJ. Seroprevalence of cytomegalovirus infection in the United States, 1988-1994. Clin Infect Dis 2006;43:1143–51.
20. Wills MR, Carmichael AJ, Mynard K, Jin X, Weekes MP, Plachter B, et al. The human cytotoxic T-lymphocyte (CTL) response to cytomegalovirus is dominated by structural protein pp65: frequency, specificity, and T-cell receptor usage of pp65-specific CTL. J Virol 1996;70:7569–79.
21. Schoenberger SP, Toes RE, van d V, Offringa R, Melief CJ. T-cell help for cytotoxic T lymphocytes is mediated by CD40-CD40L interactions. Nature 1998;393:480–3.
22. Schoenberger SP, Jonges LE, Mooijaart RJ, Hartgers F, Toes RE, Kast WM, et al. Efficient direct priming of tumor-specific cytotoxic T lymphocyte in vivo by an engineered APC. Cancer Res 1998;58:3094–100.
23. Caux C, Massacrier C, Vanbervliet B, Dubois B, Van KC, Durand I, et al. Activation of human dendritic cells through CD40 cross-linking. J Exp Med 1994;180:1263–72.
24. Evans DE, Prell RA, Thalhofer CJ, Hurwitz AA, Weinberg AD. Engagement of OX40 enhances antigen-specific CD4(+) T cell mobilization/memory development and humoral immunity: comparison of alphaOX-40 with alphaCTLA-4. J Immunol 2001;167:6804–11.
25. Weinberg AD, Evans DE, Thalhofer C, Shi T, Prell RA. The generation of T cell memory: a review describing the molecular and cellular events following OX40 (CD134) engagement. J Leukoc Biol 2004;75:962–72.
26. Gramaglia I, Jember A, Pippig SD, Weinberg AD, Killeen N, Croft M. The OX40 costimulatory receptor determines the development of CD4 memory by regulating primary clonal expansion. J Immunol 2000;165:3043–50.
27. Di Stasi A, Tey SK, Dotti G, Fujita Y, Kennedy-Nasser A, Martinez C, et al. Inducible apoptosis as a safety switch for adoptive cell therapy. N Engl J Med 2011;365:1673–83.
28. Smith CA, Ng CY, Heslop HE, Holladay MS, Richardson S, Turner EV, et al. Production of genetically modified Epstein-Barr virus-specific cytotoxic T cells for adoptive transfer to patients at high risk of EBV-associated lymphoproliferative disease. J Hematother 1995;4:73–9.
29. Vera J, Savoldo B, Vigouroux S, Biagi E, Pule M, Rossig C, et al. T lymphocytes redirected against the kappa light chain of human immunoglobulin efficiently kill mature B lymphocyte-derived malignant cells. Blood 2006;108:3890–7.
30. Naldini L, Blomer U, Gallay P, Ory D, Mulligan R, Gage FH, et al. In vivo gene delivery and stable transduction of nondividing cells by a lentiviral vector. Science 1996;272:263–7.
31. Pule MA, Straathof KC, Dotti G, Heslop HE, Rooney CM, Brenner MK. A chimeric T cell antigen receptor that augments cytokine release and supports clonal expansion of primary human T cells. Mol Ther 2005;12:933–41.
32. Koo GC, Hasan A, O'Reilly RJ. Use of humanized severe combined immunodeficient mice for human vaccine development. Expert Rev Vaccines 2009;8:113–20.
33. Perna SK, Pagliara D, Mahendravada A, Liu H, Brenner MK, Savoldo B, et al. Interleukin-7 mediates selective expansion of tumor-redirected cytotoxic T lymphocytes (CTLs) without enhancement of regulatory T-cell inhibition. Clin Cancer Res 2014;20:131–9.
34. Rabinovich BA, Ye Y, Etto T, Chen JQ, Levitsky HI, Overwijk WW, et al. Visualizing fewer than 10 mouse T cells with an enhanced firefly luciferase in immunocompetent mouse models of cancer. Proc Natl Acad Sci U S A 2008;105:14342–6.
35. Tey SK, Dotti G, Rooney CM, Heslop HE, Brenner MK. Inducible caspase 9 suicide gene to improve the safety of allodepleted T cells after haploidentical stem cell transplantation. Biol Blood Marrow Transplant 2007;13:913–24.
36. Kutzler MA, Weiner DB. DNA vaccines: ready for prime time? Nat Rev Genet 2008;9:776–88.
37. Kenter GG, Welters MJ, Valentijn AR, Lowik MJ, Berends-van der Meer DM, Vloon AP, et al. Vaccination against HPV-16 oncoproteins for vulvar intraepithelial neoplasia. N Engl J Med 2009;361:1838–47.
38. Kantoff PW, Higano CS, Shore ND, Berger ER, Small EJ, Penson DF, et al. Sipuleucel-T immunotherapy for castration-resistant prostate cancer. N Engl J Med 2010;363:411–22.
39. McConkey SJ, Reece WH, Moorthy VS, Webster D, Dunachie S, Butcher G, et al. Enhanced T-cell immunogenicity of plasmid DNA vaccines boosted by recombinant modified vaccinia virus Ankara in humans. Nat Med 2003;9:729–35.
40. Wu Y, Ellis RD, Shaffer D, Fontes E, Malkin EM, Mahanty S, et al. Phase 1 trial of malaria transmission blocking vaccine candidates Pfs25 and Pvs25 formulated with montanide ISA 51. PLoS One 2008;3:e2636.
41. Salgia R, Lynch T, Skarin A, Lucca J, Lynch C, Jung K, et al. Vaccination with irradiated autologous tumor cells engineered to secrete granulocyte-macrophage colony-stimulating factor augments antitumor immunity in some patients with metastatic non-small-cell lung carcinoma. J Clin Oncol 2003;21:624–30.
42. Bowman L, Grossmann M, Rill D, Brown M, Zhong WY, Alexander B, et al. IL-2 adenovector-transduced autologous tumor cells induce antitumor immune responses in patients with neuroblastoma. Blood 1998;92:1941–9.
43. Biagi E, Rousseau R, Yvon E, Schwartz M, Dotti G, Foster A, et al. Responses to human CD40 ligand/human interleukin-2 autologous cell vaccine in patients with B-cell chronic lymphocytic leukemia. Clin Cancer Res 2005;11(19 Pt 1):6916–23.
44. Rousseau RF, Biagi E, Dutour A, Yvon ES, Brown MP, Lin T, et al. Immunotherapy of high-risk acute leukemia with a recipient (autologous) vaccine expressing transgenic human CD40L and IL-2 after chemotherapy and allogeneic stem cell transplantation. Blood 2006;107:1332–41.
45. Wierda WG, Cantwell MJ, Woods SJ, Rassenti LZ, Prussak CE, Kipps TJ. CD40-ligand (CD154) gene therapy for chronic lymphocytic leukemia. Blood 2000;96:2917–24.
46. Chiodoni C, Paglia P, Stoppacciaro A, Rodolfo M, Parenza M, Colombo MP. Dendritic cells infiltrating tumors cotransduced with granulocyte/macrophage colony-stimulating factor (GM-CSF) and CD40 ligand genes take up and present endogenous tumor-associated antigens, and prime naive mice for a cytotoxic T lymphocyte response. J Exp Med 1999;190:125–33.
47. Biagi E, Dotti G, Yvon E, Lee E, Pule M, Vigouroux S, et al. Molecular transfer of CD40 and OX40 ligands to leukemic human B cells induces expansion of autologous tumor-reactive cytotoxic T lymphocytes. Blood 2005;105:2436–42.
48. Sugamura K, Ishii N, Weinberg AD. Therapeutic targeting of the effector T-cell co-stimulatory molecule OX40. Nat Rev Immunol 2004;4:420–31.
49. Weinberg AD. OX40: targeted immunotherapy–implications for tempering autoimmunity and enhancing vaccines. Trends Immunol 2002;23:102–9.

Published OnlineFirst February 17, 2015; DOI: 10.1158/1078-0432.CCR-14-2998

Clinical Cancer Research

K562-Derived Whole-Cell Vaccine Enhances Antitumor Responses of CAR-Redirected Virus-Specific Cytotoxic T Lymphocytes *In Vivo*

Ignazio Caruana, Gerrit Weber, Brandon C. Ballard, et al.

Clin Cancer Res 2015;21:2952-2962. Published OnlineFirst February 17, 2015.

nature medicine

Heparanase promotes tumor infiltration and antitumor activity of CAR-redirected T lymphocytes

Ignazio Caruana[1], Barbara Savoldo[1,2], Valentina Hoyos[1], Gerrit Weber[1], Hao Liu[3], Eugene S Kim[4], Michael M Ittmann[5–7], Dario Marchetti[5] & Gianpietro Dotti[1,5,8]

Adoptive transfer of chimeric antigen receptor (CAR)-redirected T lymphocytes (CAR-T cells) has had less striking therapeutic effects in solid tumors[1–3] than in lymphoid malignancies[4,5]. Although active tumor-mediated immunosuppression may have a role in limiting the efficacy of CAR-T cells[6], functional changes in T lymphocytes after their *ex vivo* manipulation may also account for the reduced ability of cultured CAR-T cells to penetrate stroma-rich solid tumors compared with lymphoid tissues. We therefore studied the capacity of human *in vitro*–cultured CAR-T cells to degrade components of the extracellular matrix (ECM). In contrast to freshly isolated T lymphocytes, we found that *in vitro*–cultured T lymphocytes lack expression of the enzyme heparanase (HPSE), which degrades heparan sulfate proteoglycans, the main components of ECM. We found that *HPSE* mRNA is downregulated in *in vitro*–expanded T cells, which may be a consequence of *p53* (officially known as *TP53*, encoding tumor protein 53) binding to the *HPSE* gene promoter. We therefore engineered CAR-T cells to express HPSE and showed their improved capacity to degrade the ECM, which promoted tumor T cell infiltration and antitumor activity. The use of this strategy may enhance the activity of CAR-T cells in individuals with stroma-rich solid tumors.

CAR-T cells in *in vitro* cultures consist mostly of memory and effector lymphocytes characterized by potent cytotoxic function[1,4,7]. However, to exploit their effector functions *in vivo*, CAR-T cells must traffic to and accumulate in tumor sites. These processes involve a complex sequence of events, beginning with the adhesion of T cells to endothelial cells and followed by chemokine-chemokine receptor interactions, that modulates their extravasation into antigen-rich tissues[8–10]. During this process, T lymphocytes actively degrade the main components of the subendothelial basement membrane and the ECM, including the heparan sulfate proteoglycans (HSPGs)[11]. The ECM is an integral component of the stroma, and therefore T cells attacking stroma-rich solid tumors must be able to degrade HSPGs in order to access tumor cells and exert antitumor effects.

The release of specific enzymes by T cells is fundamental to the degradation of ECM. One of these enzymes is HPSE, which is the only known mammalian β-D-endoglycosidase capable of cleaving the heparan sulfate chains of HSPGs[9,12–14]. HPSE is first synthesized as a latent precursor protein of ~65 kDa and then cleaved into two subunits of ~8 and ~50 kDa that heterodimerize to form the enzymatically active protein[13]. HPSE is produced in large amounts by activated $CD4^+$ T lymphocytes, neutrophils, monocytes and B lymphocytes[15–17]. However, the exact contribution of HPSE in mediating the tumor infiltration of *in vitro*–cultured, tumor-specific T cells remains unexplored.

We first assessed whether *ex vivo*–expanded human T cells are defective in their capacity to degrade the ECM. Using a Matrigel-based cell invasion assay, we compared the invasion capacity of freshly isolated resting T cells (FI-T cells), briefly activated T cells (BA-T cells; 24 h of activation with CD3-specific (OKT3) and CD28-specific antibodies) and long-term *ex vivo*–expanded T cells (LTE-T cells; activation with OKT3 and CD28-specific antibodies and *ex vivo* culture for 12–14 d). Consistent with previously reported data in rodents[12], BA-T cells showed superior invasion of the ECM compared to FI-T cells (34% ± 8% vs. 23% ± 8%, respectively; $P = 0.05$). Conversely, LTE-T cells had a significantly reduced ability to degrade ECM (8% ± 6%) compared to both BA-T ($P = 0.01$) and FI-T ($P = 0.022$) cells (**Fig. 1a**). To dissect the mechanisms responsible for this observation, we evaluated the expression and function of HPSE in each cell population. In accordance with the cell invasion assay, both $CD4^+$ and $CD8^+$ T cells from FI-T and BA-T cells retained the active form of HPSE (50 kDa), whereas the enzyme was not detectable by western blotting and immunofluorescence in LTE-T cells (**Fig. 1b**,**c**). The loss of HPSE expression in LTE-T cells was not determined by the culture medium or cytokines used for T cell growth, as we observed similar results using either human type AB serum or fetal bovine serum, and interleukin (IL)-2, IL-7 or IL-15 as T cell growth factors (**Supplementary Fig. 1**). We also found that the loss of HPSE expression in response to stimulation with OKT3 and anti-CD28 antibodies and cytokines is observed in naive ($CD45RA^+$), central memory

[1]Center for Cell and Gene Therapy, Baylor College of Medicine and Houston Methodist Hospital, Houston, Texas, USA. [2]Department of Pediatrics, Texas Children's Hospital, Baylor College of Medicine, Houston, Texas, USA. [3]Biostatistics Shared Resource, Baylor College of Medicine, Houston, Texas, USA. [4]Department of Surgery, Texas Children's Hospital, Baylor College of Medicine, Houston, Texas, USA. [5]Department of Pathology and Immunology, Baylor College of Medicine, Houston, Texas, USA. [6]Interdepartmental Program in Translational Biology and Molecular Medicine, Baylor College of Medicine, Houston, Texas, USA. [7]Michael E. DeBakey Department of Veterans Affairs Medical Center, Dan L. Duncan Cancer Center, Houston, Texas, USA. [8]Department of Medicine, Baylor College of Medicine, Houston, Texas, USA. Correspondence should be addressed to G.D. (gdotti@bcm.edu).

Received 23 November 2014; accepted 27 February 2015; published online 13 April 2015; doi:10.1038/nm.3833

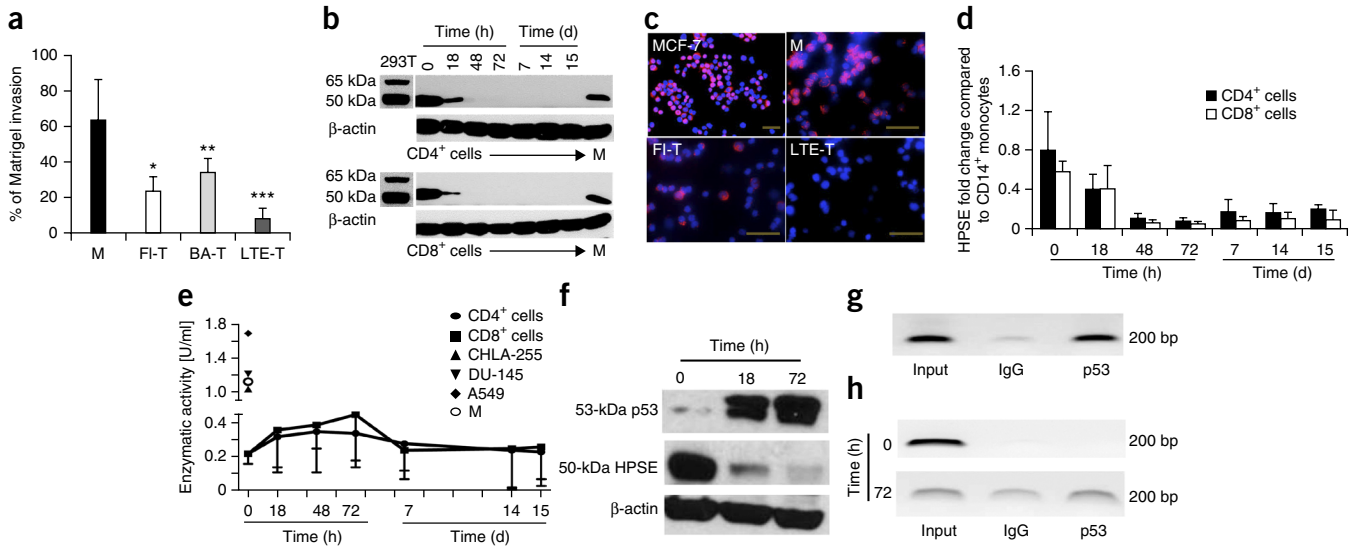

Figure 1 LTE-T cells show reduced invasion of the ECM and loss of the enzyme HPSE. (**a**) ECM invasion assay of CD14+ monocytes (M), FI-T cells, BA-T cells and LTE-T cells. Monocytes freshly isolated from peripheral blood showed the highest capacity to degrade the ECM (63% ± 23%). BA-T cells showed superior invasion of ECM compared to FI-T cells (**$P = 0.05$) and LTE-T cells (***$P = 0.01$), while LTE-T cells also showed inferior invasion compared to FI-T cells (*$P = 0.022$); analysis of variance (ANOVA) followed by a log-rank (Mantel–Cox) test for multiple comparisons. Data summarize means ± s.d. of five donors. We compared all four cell subsets for each donor. (**b**) Western blot showing the expression of HPSE in monocytes (M), CD4+ and CD8+ T cells at different culture time points. Data are representative of four donors. Positive controls are *HPSE*-transfected 293T cells. (**c**) Immunofluorescence staining for HPSE in MCF-7 cells, M, FI-T cells and LTE-T cells. Nuclei are stained with DAPI and shown in blue, whereas HPSE is stained with red fluorescent dye (Alexa Fluor 555). Magnification is 20×; scale bars, 50 µm. (**d**) qRT-PCR of *HPSE* in CD4+ and CD8+ T cells at different culture time points. Data summarize means ± s.d. of four donors. (**e**) HPSE enzymatic activity assessed in supernatants collected from CD4+ and CD8+ T cells at different culture time points. Monocytes and tumor cell lines CHLA-255, A549 and DU-145 are positive controls. Data summarize means ± s.d. of 4 donors. In **b**,**d**,**e** the condition 'day 15' indicates HPSE expression in LTE-T cells cultured for 14 d and re-stimulated with immobilized OKT3 and CD28-specific antibodies for 24 h to assess whether TCR re-stimulation can re-induce HPSE expression. (**f**) Western blot showing the expression of HPSE and full-length p53 protein in T cells before ($t = 0$) and after activation with immobilized OKT3 and CD28-specific antibodies for 18 and 72 h. Shown are results from one representative of three donors. (**g**,**h**) p53 ChIP in LTE-T cells cultured for 14 d (**g**), and in CD45RA+ cells before ($t = 0$) and after stimulation with OKT3 and CD28-specific monoclonal antibodies ($t = 72$ h) (**h**). Input is DNA that has been sonicated but not immunoprecipitated; IgG and p53 are DNA immunoprecipitated by the isotype and p53-specific antibody that recognizes the full-length protein. Relative quantification was performed comparing the intensities of PCR bands of IgG and p53 to input PCR band. For this representative sample, relative quantifications are: IgG, 20% and p53, 90% for LTE-T cells (**g**); IgG, 2% and p53, 4% at $t = 0$ and IgG, 53% and p53, 100% at $t = 72$ h for CD45RA+ cells (**h**). Shown is one representative of three donors.

(CD45RO+CD62L+) and effector memory (CD45RO+CD62L−) T cells isolated from the peripheral blood, suggesting that this is a general phenomenon and that it is not T cell subset specific (**Supplementary Fig. 2**). The absence of HPSE protein in LTE-T cells was associated with the downregulation of the *HPSE* mRNA. As shown in **Figure 1d**, *HPSE* mRNA decreased immediately after activation in both CD4+ and CD8+ T cells compared to CD14+ monocytes ($P < 0.005$ and $P < 0.031$, respectively) and remained low over the subsequent 14 d of culture. Re-stimulation of LTE-T cells with OKT3 and anti-CD28 antibodies on day 14 of culture did not induce re-expression of either the *HPSE* mRNA or protein (**Fig. 1b**,**d**). The lack of cellular HPSE in LTE-T cells was also confirmed by the absence of enzymatic activity in the culture supernatant. As shown in **Figure 1e**, HPSE enzymatic activity was detected in supernatants collected within the first 72 h after activation of FI-T cells. This detection can be attributed to enzyme accumulation in the culture medium. However, the enzymatic activity returned to background levels 72 h later (from 0.34 ± 0.2 U ml and 0.45 ± 0.27 U ml to 0.22 ± 0.06 U ml) for both CD4+ and CD8+ T cells (**Fig. 1e**). This observation is in line with previous studies reporting that preformed HPSE protein is stored in an intracellular compartment and released as an early event in response to T cell activation[18]. We found that HPSE is also absent in Epstein–Barr virus–specific cytotoxic T cells that are stimulated *in vitro* by antigen-presenting cells, suggesting that HPSE loss in LTE-T cells is not caused by a supra-physiological activation of these cells mediated by OKT3 antibody[19] (**Supplementary Fig. 2**). Previous studies showed that mutated *p53* with loss of function in tumor cells is associated with overexpression of HPSE[20]. Because there is an accumulation of full-length p53 in LTE-T cells[20,21], we suggest that the lack of *HPSE* mRNA expression in LTE-T cells may be due to the accumulation of full-length p53 in LTE-T cells, which binds to the *HPSE* gene promoter (**Fig. 1f–h** and **Supplementary Fig. 3**). The immediate translational implication of these findings is that T cells that are engineered *in vitro* and cultured for adoptive immunotherapy lack HPSE expression when infused into subjects, and they are thus impaired in their capacity to degrade components of the ECM of the stroma. It is also important to note that the cleavage of HPSG chains by HPSE releases preformed stored chemokines into the stroma[22,23]. Because chemokines also guide the migration of T cells toward their target cells within the tumor microenvironment, the lack of HPSE may further indirectly compromise the antitumor effects of T cells by reducing their migration.

We thus hypothesized that engineering LTE-T cells to express HPSE through retroviral gene transfer would improve their invasion capability. LTE-T cells transduced with the HPSE(I)GFP retroviral vector expressed GFP (**Fig. 2a**) and HPSE (**Fig. 2b**). HPSE expression

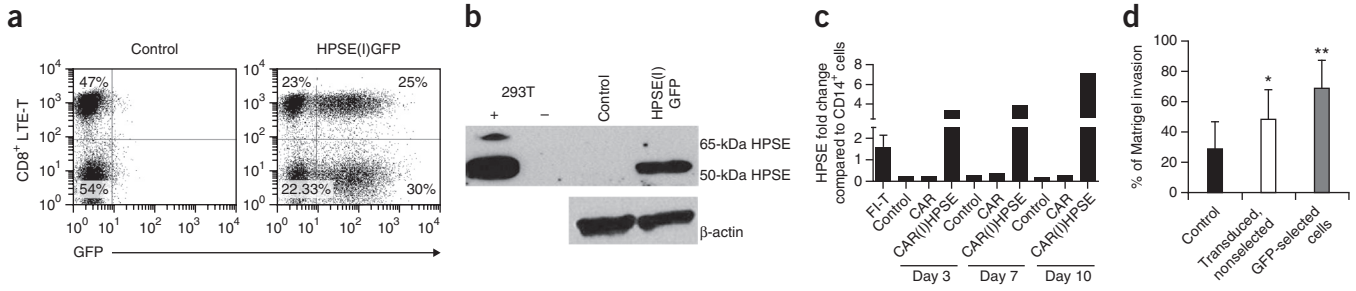

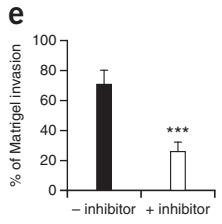

Figure 2 LTE-T cells modified to express HPSE show enhanced degradation of the ECM. We transduced LTE-T cells with retroviral vectors encoding *HPSE* and GFP (HPSE(I)GFP) or both the GD2-specific CAR and *HPSE* (CAR(I)HPSE). (**a**) GFP expression by both CD4$^+$ and CD8$^+$ LTE-T cells at days 12–14 of culture. (**b**) Western blot showing the expression of HPSE in control and transduced LTE-T cells at days 12–14 of culture. (**c**) qRT-PCR of *HPSE* in control and CAR(I)HPSE$^+$ LTE-T cells cultured in IL-2 deficient medium for 3, 7 and 10 d. Data are representative of two donors. (**d**) HPSE(I)GFP$^+$ LTE-T cells were sorted based on GFP expression. After sorting we used the ECM invasion assay to compare control, nonsorted HPSE(I)GFP$^+$ LTE-T cells and GFP-sorted HPSE(I)GFP$^+$ LTE-T cells. Data summarize mean ± s.d. of nine donors, $^*P = 0.025$; $^{**}P < 0.001$. (**e**) ECM invasion assay of *HPSE*-transduced LTE-T cells in the presence or absence of the inhibitor heparin H1. Data summarize mean ± s.d. of four donors, $^{***}P < 0.01$; Student's *t*-test.

remained high in transduced LTE-T cells starved of cytokines in culture for more than 10 d, suggesting stable transgene expression (**Fig. 2c**). In functional assays, HPSE(I)GFP$^+$ LTE-T cells better degraded ECM (48% ± 19%) than did control untransduced LTE-T cells (29% ± 18%; $P = 0.025$) (**Fig. 2d**). The addition of the HPSE inhibitor heparin H1 (ref. 24) confirmed that the invasion of HPSE(I)GFP$^+$

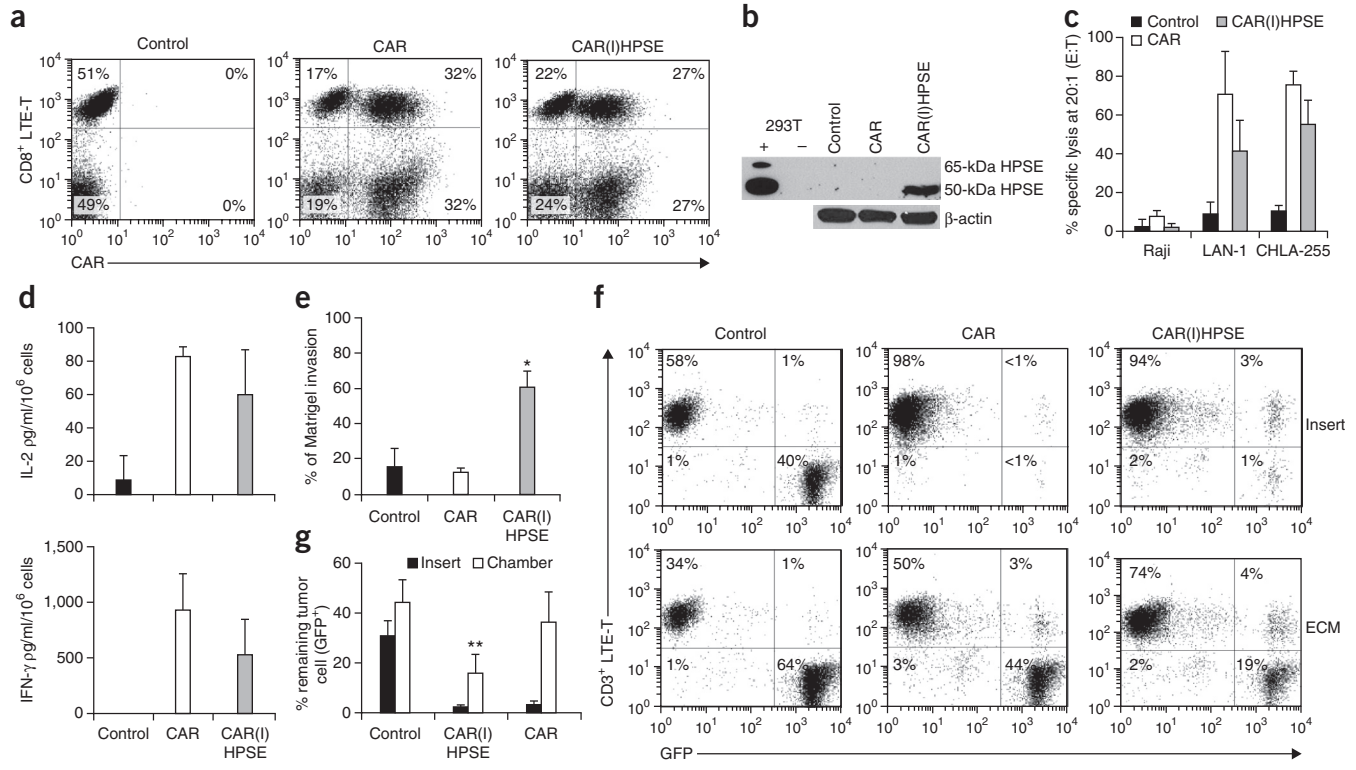

Figure 3 LTE-T cells co-expressing *HPSE* and GD2-specific CAR retain GD2 specificity and have enhanced capacity to degrade ECM. We transduced LTE-T cells with retroviral vectors encoding either the GD2-specific CAR alone (CAR) or both the GD2-specific CAR and *HPSE* (CAR(I)HPSE). (**a**) Flow cytometry analysis to detect CAR expression by control and transduced LTE-T cells. (**b**) Western blot to detect HPSE in control and transduced LTE-T cells. Data are representative of five donors. (**c**) Cytotoxic activity of control, CAR$^+$ and CAR(I)HPSE$^+$ LTE-T cells assessed by ^{51}Cr-release assay at a 20:1 E:T ratio. We used LAN-1 and CHLA-255 cells (GD2$^+$), and Raji cells (GD2$^-$) as target cells. (**d**) Transduced LTE-T cells release both IL-2 and IFN-γ in response to GD2$^+$ tumor cells. (**e**) Invasion of ECM by control, CAR$^+$ and CAR(I)HPSE$^+$ LTE-T cells. Data in **c**–**e** summarize mean ± s.d. from five donors, $^*P = 0.004$; Student's *t*-test. (**f**,**g**) We plated control and transduced LTE-T cells in the upper chamber of the Matrigel invasion assay either with ECM or without ECM (insert), and LAN-1-GFP$^+$ cells in the lower chamber. After day 3 of culture, we collected cells in the lower chamber to quantify CD3$^+$ T cells and GFP$^+$ tumor cells by flow cytometry. (**f**) illustrates representative dot plots of the flow cytometry of CD3$^+$ T cells versus GFP$^+$ tumor cells, whereas (**g**) summarizes mean ± s.d. of residual GFP$^+$ tumor cells of five donors, $^{**}P = 0.009$. In all cases we analyzed LTE-T cells by days 12–14 of culture.

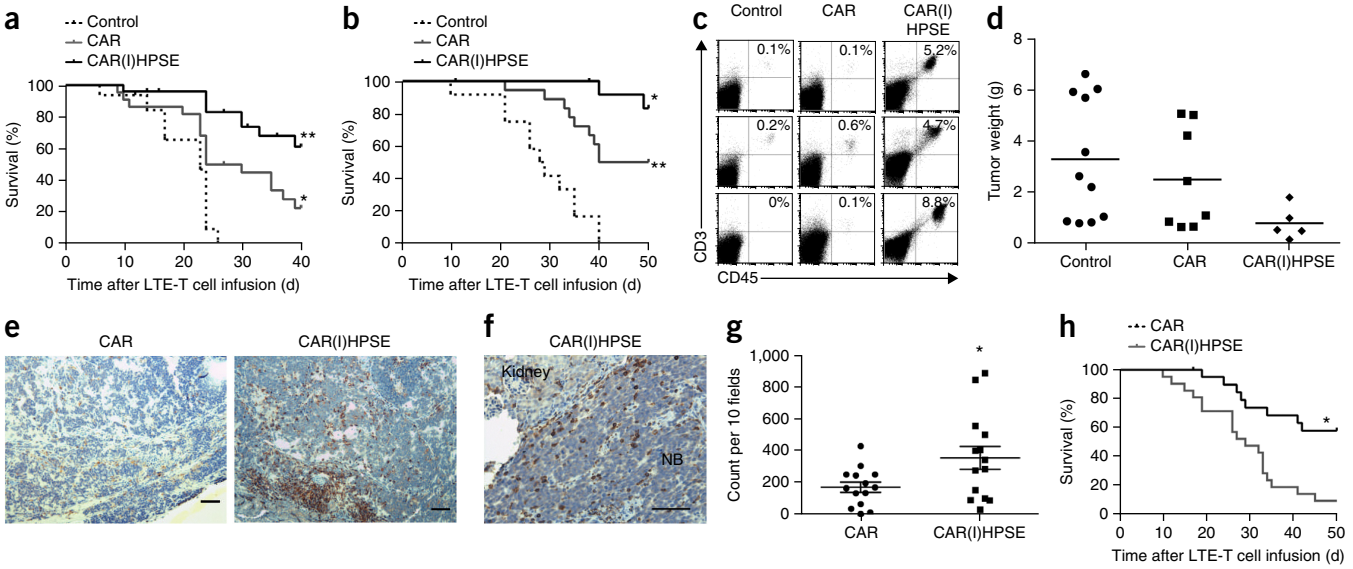

Figure 4 CAR-GD2$^+$ LTE-T cells co-expressing *HPSE* show enhanced tumor infiltration and improve overall survival in xenograft tumor models. (**a**) Kaplan–Meier analysis of mice engrafted i.p. with the tumor cell line CHLA-255 and treated i.p. with control, CAR$^+$ and CAR(I)HPSE$^+$ LTE-T cells. Shown are data from three independent experiments using LTE-T cells generated from three donors. Control, $n = 16$; CAR, $n = 22$; CAR(I)HPSE, $n = 26$ mice; $^*P < 0.007$, $^{**}P < 0.0001$. (**b**) Kaplan–Meier analysis of mice engrafted i.p. with the tumor cell line LAN-1 and treated i.p. with control, CAR$^+$ and CAR(I)HPSE$^+$ LTE-T cells. For these experiments, we generated LTE-T cells from two donors. Control, $n = 12$; CAR, $n = 18$; CAR(I)HPSE, $n = 14$ mice; $^*P = 0.039$, $^{**}P < 0.0001$. (**c**) Flow cytometry analysis of CD3$^+$ T cells detected within the tumor samples. Dot plots are representative of three mice per group from mice infused with LTE-T cells generated from the same donor. (**d**) Weight of the tumors collected from euthanized mice engrafted with LAN-1 tumor cells. (**e**,**f**) Immunohistochemical analysis showing CD3$^+$ T cell infiltration in NB tumor CHLA-255 cells implanted in the kidney of mice infused with either CAR$^+$ or CAR(I)HPSE$^+$ LTE-T cells. 100× magnification (**e**) and 200× magnification (**f**); scale bars, 100 µm. (**g**) The graph shows the numbers of infiltrating CD3$^+$ T cells per ten high-power fields in tumors collected from mice treated with either CAR$^+$ or CAR(I)HPSE$^+$ LTE-T cells (cell numbers 357 ± 72 and 173 ± 32, respectively), $^*P = 0.028$. (**h**) Kaplan-Meier analysis of mice surgically implanted under the renal capsule with CHLA-255 NB cells and infused i.v. with either CAR$^+$ or CAR(I)HPSE$^+$ LTE-T cells. For these experiments, we generated LTE-T cells from two donors, CAR, $n = 21$; CAR(I)HPSE, $n = 21$ mice; $^*P = 0.0006$.

LTE-T cells is HPSE-specific, as invasion was reduced from 74% ± 14% in the absence of inhibitor to 29% ± 9% ($P < 0.01$) in the presence of heparin H1 (**Fig. 2e**). We then assessed whether HPSE expression leading to improved cell invasion could be coupled with antitumor specificity. We used neuroblastoma (NB) as a cancer model because this tumor type has been targeted in a clinical trial with a CAR specific to the NB-associated antigen GD2 with some clinical responses[1]. On day 14 of culture, CAR expression was 71% ± 14% and 56% ± 6% in LTE-T cells transduced with CAR and CAR(I)HPSE vectors, respectively (**Fig. 3a**). HPSE was detected only in LTE-T cells transduced with the CAR(I)HPSE vector (**Fig. 3b**). Both CAR$^+$ and CAR(I)HPSE$^+$ LTE-T cells lysed the GD2$^+$ human NB cell line LAN-1 (71% ± 22% and 41% ± 16%, respectively, at a 20:1 effector-to-target cell (E:T) ratio in a ^{51}Cr-release assay)(P = nonsignificant (ns)), and the GD2$^+$ human NB cell line CHLA-255 (76% ± 7% and 55% ± 13%, respectively) (P = ns), whereas both CAR$^+$ and CAR(I)HPSE$^+$ LTE-T cells showed negligible activity against the GD2$^-$ Raji cell line (<8%) (**Fig. 3c**). Control LTE-T cells lacking the CAR lysed none of these targets. The cytolytic activity was associated with a preserved T_H1 cytokine profile, as CAR$^+$ and CAR(I)HPSE$^+$ LTE-T released similar amounts of interferon (IFN)-γ (927 ± 328 and 527 ± 320 pg/ml × 10^6 cells, respectively; P = ns) and IL-2 (83 ± 6 and 61 ± 27 pg/ml × 10^6 cells, respectively, P = ns) in response to stimulation with GD2$^+$ tumor cells (**Fig. 3d**). In sharp contrast to their comparable cytolytic function, only CAR(I)HPSE$^+$ LTE-T cells degraded the ECM (66% ± 1%) compared to CAR$^+$ or control LTE-T cells (13% ± 9% and 16% ± 10%, respectively) ($P = 0.004$ and $P < 0.001$) (**Fig. 3e**). To prove *ex vivo* that LTE-T cells co-expressing *HPSE* and CAR have increased antitumor activity in the presence of ECM, we plated LTE-T and tumor cells in a Matrigel cell invasion assay, in which LTE-T cells must degrade the ECM to reach and eliminate the tumor targets. After 3 d of culture, both CAR$^+$ and CAR(I)HPSE$^+$ LTE-T cells eliminated LAN-1 tumor cells equally well in the absence of the ECM (<3% GFP$^+$ tumor cells) compared to control LTE-T cells (31% ± 6% GFP$^+$ tumor cells) (**Fig. 3f**,**g**). By contrast, in the presence of ECM, CAR(I)HPSE$^+$ LTE-T cells eliminated all but 16% ± 8% of LAN-1 cells, compared to 37% ± 12% in the presence of CAR$^+$ LTE-T cells ($P = 0.001$) (**Fig. 3f**,**g**). Control LTE-T cells did not show antitumor activity (45% ± 9% GFP$^+$ tumor cells). We obtained identical results with the CHLA-255 human NB cell line (**Supplementary Fig. 4**). Thus, only LTE-T cells co-expressing *HPSE* and CAR show robust antitumor activity in the presence of the ECM. The improved antitumor activity of CAR(I)HPSE$^+$ LTE-T cells was achieved without causing detectable detrimental effects on T lymphocytes. Indeed, CAR(I)HPSE$^+$ LTE-T cells expanded *in vitro*, retained the same phenotype of CAR$^+$ LTE-T cells and did not show increased activation-induced cell death in response to either OKT3-specific antibody, which binds CD3, or 1A7 anti-idiotype antibody, which causes cross-linking of the GD2-specific CAR[1] (**Supplementary Fig. 5**).

To validate our findings *in vivo*, we first established xenograft models of NB by implanting NSG-strain mice intraperitoneally (i.p.) with either CHLA-255 or LAN-1 NB cell lines in the presence of Matrigel to allow the formation of complex and structured tumors. We used the i.p. route to minimize confounding variables related to T cell homing to the tumor, a known issue in NB xenograft models when the tumor is inoculated subcutaneously[25]. After 10 d, mice received

either control, CAR+ or CAR(I)HPSE+ LTE-T cells i.p. As shown in **Figure 4a**, mice implanted with CHLA-255 tumor cells and treated with CAR(I)HPSE+ LTE-T cells had significantly improved survival by day 40 compared to mice treated with control LTE-T ($P < 0.001$) or CAR+ LTE-T ($P < 0.007$) cells. Among treated mice, we found that 6 of 22 infused with CAR+ LTE-T cells, and 18 of 26 infused with CAR(I)HPSE+ LTE-T cells were macroscopically tumor free when we ended the observation at day 40 ($P = 0.008$). We obtained similar results in mice engrafted with LAN-1 tumor cells. Mice infused with CAR(I)HPSE+ LTE-T cells had significantly improved survival compared to mice treated with control ($P < 0.0001$) or CAR+ LTE-T cells at day 50 ($P < 0.039$) (**Fig. 4b** and **Supplementary Fig. 6**). In another set of experiments, we euthanized mice on day 12–14 after T cell infusion to measure tumor T cell infiltration. Tumors collected from mice infused with CAR(I)HPSE+ LTE-T cells had greater T cell infiltration (4.6% ± 2.4%) compared to those treated with control (0.6% ± 0.5; $P = 0.029$) or CAR+ LTE-T cells (0.1% ± 0.1; $P = 0.043$) (**Fig. 4c**). Tumors collected from euthanized mice also showed a significant reduction in weight in recipients infused with CAR(I)HPSE+ LTE-T cells compared to control (0.8 g ± 0.6 g vs. 3.3 g ± 2.4 g) ($P = 0.039$), and when compared to mice infused with CAR+ LTE-T cells (0.8 g ± 0.6 g vs. 2.5 g ± 2 g), although this difference was not statistically significant ($P = 0.093$) (**Fig. 4d**). Because NB cell lines require Matrigel to form complex and structured tumors when infused i.p., we also implemented a third NB model in which CHLA-255 tumor cells labeled with firefly luciferase were implanted in the kidney of Nod scid gamma (NSG) mice without using Matrigel[26], and CAR+ LTE-T and CAR(I)HPSE+ LTE cells were infused intravenously (i.v.). Tumor sections from mice infused i.v. with CAR(I)HPSE+ LTE-T cells showed enhanced infiltration of CD3+ T cells compared to CAR+ LTE-T cells (357 ± 72 and 173 ± 32 cells, respectively; $P = 0.028$) (**Fig. 4e–g**). Long-term observation of infused mice also showed improved survival of recipients treated with CAR(I)HPSE+ LTE-T cells by day 50 ($P < 0.005$) (**Fig. 4h** and **Supplementary Fig. 6**).

Finally, we extended our observation to CAR+ LTE-T cells targeting the solid tumor-associated antigen chondroitin sulfate proteoglycan 4 (CSPG4)[27] in an aggressive melanoma model, suggesting that the positive effect of HPSE in CAR-T cells can be extrapolated to other targeted antigens and solid tumors (**Supplementary Fig. 7**). In contrast, the co-expression of HPSE in LTE-T cells redirected with a CD19-specific CAR did not seem to have a role in B-lymphoid malignancies, which are generally stroma-poor compared to solid tumors (**Supplementary Fig. 8**).

Under physiological conditions, HPSE expression by T cells is regulated to avoid tissue damage from T cell extravasation into nonpathologic tissues[16,17,28,29]. To rule out concerns about non-specific infiltration of normal tissues, such as lung or liver, by *HPSE*-engineered LTE-T cells, we evaluated *in vivo* T cell biodistribution. For these experiments, we labeled CAR(I)HPSE+ and CAR+ LTE-T cells with the vector encoding GFP and firefly luciferase and infused them via tail injection. T cell biodistribution evaluated by *in vivo* imaging at different time points after T cell inoculation and immunohistochemical analysis at early and late passages did not show differences between the two groups of mice, suggesting no preferential accumulation in lung or liver of *HPSE*-engineered LTE-T cells (**Supplementary Fig. 9a**,**b**).

In conclusion, HPSE deficiency in *in vitro*–engineered and cultured tumor-specific LTE-T cells may limit their antitumor activity in stroma-rich solid tumors. Other enzymes such as matrix metalloproteases (MMPs) are also involved in modifications of ECM components and may compensate for HPSE deficiency[30]. However, we found that some MMPs are also downregulated upon TCR activation and cytokine exposure (**Supplementary Fig. 10a**,**b**). We thus suggest that inducing expression of HPSE in LET-T cells co-expressing a tumor-specific CAR improves their capacity to degrade the ECM without compromising their viability, expansion or effector function, and it promotes increased antitumor activity. The proposed strategy may enhance the antitumor activity of CAR-redirected T cells in subjects with stroma-rich solid tumors.

METHODS

Methods and any associated references are available in the online version of the paper.

Note: Any Supplementary Information and Source Data files are available in the online version of the paper.

ACKNOWLEDGMENTS

The authors would like to thank I.Vlodavsky and M. Brenner for the critical review of the manuscript and C. Gillespie for editing. This work was supported in part by the US National Institutes of Health-National Cancer Institute (G.D., no. R01 CA142636) and by a Department of Defense and Technology and Therapeutic Development Award (G.D., no. W81XWH-10-10425). L. Metelitsa kindly provided the CHLA-255 human NB cell line.

AUTHOR CONTRIBUTIONS

G.D., I.C. and B.S. designed experiments; I.C., V.H., G.W. and E.S.K. performed the experiments; I.C., B.S. and G.D. analyzed the data; I.C. and G.D. wrote the manuscript; H.L. performed the statistical analysis; M.M.I. performed the pathology; D.M. provided his expertise in the heparanase field and provided crucial reagents; all the authors reviewed and approved the final version of the manuscript.

COMPETING FINANCIAL INTERESTS

The authors declare competing financial interests: details are available in the online version of the paper.

1. Pule, M.A. *et al.* Virus-specific T cells engineered to coexpress tumor-specific receptors: persistence and antitumor activity in individuals with neuroblastoma. *Nat. Med.* **14**, 1264–1270 (2008).
2. Kershaw, M.H. *et al.* A phase I study on adoptive immunotherapy using gene-modified T cells for ovarian cancer. *Clin. Cancer Res.* **12**, 6106–6115 (2006).
3. Bawley, V.S. *et al.* T cells redirected against HER2 for adoptive immunotherapy for HER2-positive osteosarcoma. *Cancer Res.* **72**, 3500 (2012).
4. Kalos, M. *et al.* T cells with chimeric antigen receptors have potent antitumor effects and can establish memory in patients with advanced leukemia. *Sci. Transl. Med.* **3**, 95ra73 (2011).
5. Brentjens, R.J. *et al.* CD19-targeted T cells rapidly induce molecular remissions in adults with chemotherapy-refractory acute lymphoblastic leukemia. *Sci. Transl. Med.* **5**, 177ra38 (2013).
6. Zou, W. Immunosuppressive networks in the tumour environment and their therapeutic relevance. *Nat. Rev. Cancer* **5**, 263–274 (2005).
7. Savoldo, B. *et al.* CD28 costimulation improves expansion and persistence of chimeric antigen receptor-modified T cells in lymphoma patients. *J. Clin. Invest.* **121**, 1822–1826 (2011).
8. Muller, W.A. Leukocyte-endothelial-cell interactions in leukocyte transmigration and the inflammatory response. *Trends Immunol.* **24**, 327–334 (2003).
9. Parish, C.R. The role of heparan sulphate in inflammation. *Nat. Rev. Immunol.* **6**, 633–643 (2006).
10. Yadav, R., Larbi, K.Y., Young, R.E. & Nourshargh, S. Migration of leukocytes through the vessel wall and beyond. *Thromb. Haemost.* **90**, 598–606 (2003).
11. Bernfield, M. *et al.* Functions of cell surface heparan sulfate proteoglycans. *Annu. Rev. Biochem.* **68**, 729–777 (1999).
12. de Mestre, A.M., Staykova, M.A., Hornby, J.R., Willenborg, D.O. & Hulett, M.D. Expression of the heparan sulfate-degrading enzyme heparanase is induced in infiltrating CD4+ T cells in experimental autoimmune encephalomyelitis and regulated at the level of transcription by early growth response gene 1. *J. Leukoc. Biol.* **82**, 1289–1300 (2007).
13. Vlodavsky, I., Ilan, N., Naggi, A. & Casu, B. Heparanase: structure, biological functions, and inhibition by heparin-derived mimetics of heparan sulfate. *Curr. Pharm. Des.* **13**, 2057–2073 (2007).

14. Yurchenco, P.D. & Schittny, J.C. Molecular architecture of basement membranes. *FASEB J.* **4**, 1577–1590 (1990).
15. Fridman, R. *et al.* Soluble antigen induces T lymphocytes to secrete an endoglycosidase that degrades the heparan sulfate moiety of subendothelial extracellular matrix. *J. Cell. Physiol.* **130**, 85–92 (1987).
16. Naparstek, Y., Cohen, I.R., Fuks, Z. & Vlodavsky, I. Activated T lymphocytes produce a matrix-degrading heparan sulphate endoglycosidase. *Nature* **310**, 241–244 (1984).
17. Vlodavsky, I. *et al.* Expression of heparanase by platelets and circulating cells of the immune system: possible involvement in diapedesis and extravasation. *Invasion Metastasis* **12**, 112–127 (1992).
18. Bartlett, M.R., Underwood, P.A. & Parish, C.R. Comparative analysis of the ability of leucocytes, endothelial cells and platelets to degrade the subendothelial basement membrane: evidence for cytokine dependence and detection of a novel sulfatase. *Immunol. Cell Biol.* **73**, 113–124 (1995).
19. Smith, C.A. *et al.* Production of genetically modified Epstein-Barr virus-specific cytotoxic T cells for adoptive transfer to patients at high risk of EBV-associated lymphoproliferative disease. *J. Hematother.* **4**, 73–79 (1995).
20. Baraz, L., Haupt, Y., Elkin, M., Peretz, T. & Vlodavsky, I. Tumor suppressor p53 regulates heparanase gene expression. *Oncogene* **25**, 3939–3947 (2006).
21. Mondal, A.M. *et al.* p53 isoforms regulate aging- and tumor-associated replicative senescence in T lymphocytes. *J. Clin. Invest.* **123**, 5247–5257 (2013).
22. Gallagher, J.T. Heparan sulfate: growth control with a restricted sequence menu. *J. Clin. Invest.* **108**, 357–361 (2001).
23. Iozzo, R.V. Matrix proteoglycans: from molecular design to cellular function. *Annu. Rev. Biochem.* **67**, 609–652 (1998).
24. Nakajima, M., Irimura, T., Di, F.N. & Nicolson, G.L. Metastatic melanoma cell heparanase. Characterization of heparan sulfate degradation fragments produced by B16 melanoma endoglucuronidase. *J. Biol. Chem.* **259**, 2283–2290 (1984).
25. Craddock, J.A. *et al.* Enhanced tumor trafficking of GD2 chimeric antigen receptor T cells by expression of the chemokine receptor CCR2b. *J. Immunother.* **33**, 780–788 (2010).
26. Patterson, D.M., Shohet, J.M. & Kim, E.S. Preclinical models of pediatric solid tumors (neuroblastoma) and their use in drug discovery. *Curr. Protoc. Pharmacol.* **52**, 14.17.1–14.17.18 (2011).
27. Geldres, C. *et al.* T lymphocytes redirected against the chondroitin sulfate proteoglycan-4 control the growth of multiple solid tumors both *in vitro* and *in vivo*. *Clin. Cancer Res.* **20**, 962–971 (2014).
28. Arvatz, G., Barash, U., Nativ, O., Ilan, N. & Vlodavsky, I. Post-transcriptional regulation of heparanase gene expression by a 3′ AU-rich element. *FASEB J.* **24**, 4969–4976 (2010).
29. Lu, W.C., Liu, Y.N., Kang, B.B. & Chen, J.H. Trans-activation of heparanase promoter by ETS transcription factors. *Oncogene* **22**, 919–923 (2003).
30. Wilson, T.J. & Singh, R.K. Proteases as modulators of tumor-stromal interaction: primary tumors to bone metastases. *Biochim. Biophys. Acta* **1785**, 85–95 (2008).

ONLINE METHODS

Cell lines. 293T, DU-145 and CHLA-255 cell lines were cultured in IMDM (Gibco, Invitrogen, Carlsbad, CA) supplemented with 10% FBS (FBS, HyClone, Thermo Scientific, Pittsburgh, PA) and 2 mM GlutaMax (Invitrogen, Carlsbad, CA). MCF-7, Raji, K562, LAN-1, Daudi and SENMA cells were cultured in RPMI1640 (HyClone) supplemented with 10% FBS and 2 mM GlutaMax. A549 cells were cultured in DMEM (GIBCO) supplemented with 10% FBS and 2 mM GlutaMax. Cells were maintained in a humidified atmosphere containing 5% CO_2 at 37 °C. Tumor cell lines MCF-7, CHLA-255, A549 and DU-145 produced HPSE. All cell lines were routinely tested for mycoplasma and for surface expression of target antigens. Furthermore, all cell lines were authenticated except for CHLA-255, which was established from a neuroblastoma subject and SENMA, which was established in our laboratory from a melanoma subject[31]. However, we routinely verified that this line retained the surface expression of the target antigens.

Isolation and culture of primary human T lymphocytes. Peripheral blood mononuclear cells (PBMCs) were isolated from samples obtained from healthy volunteers from the protocol entitled 'Humoral and cellular immune responses to tumor-associated antigens (TAA)—healthy blood and skin donors' which is being conducted after approval by the Institutional Review Board of Baylor College of Medicine, or anonymous buffy coats (purchased as discarded material from the blood bank) of healthy donors (Gulf Coast Regional Blood Center, Houston, TX) using Lymphoprep density separation (Fresenius Kabi Norge, Oslo, Norway). Monocytes were obtained from PBMCs by positive magnetic selection with CD14 microbeads (Miltenyi Biotec, Auburn, CA). $CD8^+$ and $CD4^+$ T cells were also obtained from PBMCs by negative magnetic selection (Miltenyi Biotec). In selected experiments, naive ($CD45RA^+$), central-memory ($CD45RO^+CD62L^+$) and effector-memory ($CD45RO^+CD62L^-$) T cells were also separated from PBMC by CD45RA depletion and CD62L positive paramagnetic selection (Miltenyi Biotec). T lymphocytes were activated with immobilized OKT3 (1 μg/ml) and anti-CD28 (no. 555725, Becton Dickinson Biosciences, Franklin Lakes, NJ) (1 μg/ml) antibodies and then expanded in complete medium containing 45% RPMI 1640 and 45% Click's medium (Irvine Scientific, Santa Ana, CA, USA) supplemented with 10% FBS and 2 mM GlutaMax. Cells were fed twice a week with recombinant interleukin-2 (IL-2) (50 U mL) (Chiron Therapeutics, Emeryville, CA). We defined as FI-T cells: freshly isolated resting T cells from peripheral blood that comprise naive, effector-memory and central-memory T cells; BA-T cells: briefly activated T cells that result from incubation of FI-T with OKT3 and CD28-specific antibodies for 24 h; LTE-T cells: long-term *ex vivo* expanded T cells that result from BA-T cultured *ex vivo* for 12–14 d and consist mostly of central-memory and effector-memory T cells. At day 14 of culture, LTE-T cells were reactivated with OKT3 and CD28-specific antibodies and cultured for additional 24 h. For the experiments in which we compared the invasion capacity of FI-T versus BA-T versus LTE-T cells side by side, we obtained three separated blood draws at different time points from the donors to make LTE-T, BA-T and FI-T cells to be able to run all the samples in parallel in the invasion assay.

Cell invasion assay. The capacity of each cell subset to degrade ECM was examined *in vitro* using the BioCoat Matrigel Invasion assay (Becton Dickinson Biosciences) according to the manufacturer's instructions. Five percent FBS was used as a chemoattactant in the low chamber. All experiments were performed in duplicate. Data are expressed as the percentage of invasion through the Matrigel and the membrane relative to the migration through the control membrane (8 μm polyethylene terephthalate membrane pores). The percentage of invasion was calculated as follows: (mean of cells invading through the Matrigel chamber membrane/mean of cells migrating through the control insert membrane) × 100. In specific experiments, we simultaneously evaluated the invasion and antitumor activity of LTE-T cells. Briefly, we used the BioCoat Matrigel Invasion assay and plated LAN-1-GFP^+ or CHLA-255-GFP^+ cells (1.4×10^5) in the bottom of a 24-well plate and LTE-T cells (2.5×10^5 cells) in the upper chamber/insert. Chambers and inserts were removed 24 h later. After 3 d of culture cells were then collected from the lower chamber and quantified by flow cytometry to identify tumor cells and T cells, respectively.

Western blotting. 20 μg of proteins were resolved by SDS-PAGE and transferred to polyvinylidene difluoride membranes (Bio-Rad, Hercules, CA). The antibodies and dilutions used in these experiments were as follows: mouse anti-human HPA1-HPSE (1:100 and 1:6500 dilution, clone nos. HP130 and HP3-17, respectively) (InSight Biopharmaceuticals Ltd., Rehovot, Israel) that recognizes both the 65-kDa precursor and the 50-kDa active form of HPSE-1, rabbit anti-human HPA1 polyclonal (1:4000 dilution) (no. CLANT155, Cedarlane, Burlington, NC), mouse anti-human *p53* (1:200 dilution, clone DO-1) (Santa Cruz Biotechnology, Santa Cruz, CA) that recognizes the full-length *p53* protein, mouse anti-human β-actin (1:10000 dilution, clone C4) (Santa Cruz Biotechnology) and horseradish peroxidase–conjugated secondary antibodies (1:5,000 dilution, goat anti-mouse no. sc-2005 and goat anti-rabbit no. sc-2004) (Santa Cruz Biotechnology). Blots were then incubated with SuperSignal West Femto Maximum Sensitivity Substrate (Thermo Scientific).

Immunofluorescence. Cells were fixed with 4% paraformaldehyde. After permeabilization with 0.1% Triton X-100, cells were incubated with 5% goat serum (Cell Signaling Technology, Danvers, MA) and 1% BSA to block nonspecific binding. Cells were then stained with the primary antibody against human HPSE1 (HPA1, clone HP130) (InSight Biopharmaceuticals Ltd.) (1:100 dilution at 25 °C for 2 h). Cells were then probed with Alexa Fluor 555 goat anti-mouse secondary antibody (no. 44095, 1:500 dilution at 25 °C for 2 h) (Cell Signaling Technology). Fluorescent signals were detected using a fluorescence microscope (Olympus IX70, Leeds Instruments Inc., Irving, TX). DAPI (BioLegend, San Diego, CA) was used for nuclear staining.

RNA isolation and quantitative real-time PCR (qRT-PCR). For the qRT-PCR, 100 ng of total RNA was used to prepare cDNA (TaqMan One Step PCR Master Mix Reagents Kit) (Applied Biosystems, Carlsbad, CA). Specific primers and probes that were designed, tested, and standardized by Applied Biosystems for *HPSE* and *p53* were used (*HPSE*: Hs00935036_m1; *p53*: Hs01034249_m1). The difference in cycle threshold values (ΔCT) of *HPSE* was normalized to the ΔCT of *GAPDH* (glyceraldehyde-3-phosphate dehydrogenase, Hs99999905_m1), and the fold change in expression was expressed relative to $CD14^+$ monocytes, considered as a positive control while mesemchymal stem cells were used as a negative control. For *p53* mRNA quantification the difference in cycle threshold values (ΔCt) of *p53* was normalized to the ΔCt of *GAPDH* (glyceraldehyde-3-phosphate dehydrogenase, Hs99999905_m1), and the fold change in expression was expressed relative to FI-T cells.

Enzyme-linked immunosorbent assay (ELISA). Cytokine release by LTE-T cells in response to stimulation with $GD2^+$ LAN-1 cells was analyzed using IFN-γ and IL-2–specific ELISAs (R&D Systems, Minneapolis, MN). HPSE activity was measured using a heparan sulfate (HS) degrading enzyme assay kit (Takara Bio Inc., Otsu, Shiga, Japan). HPSE activity was measured in supernatants collected at different time point of culture of T lymphocytes. At days 4 and 14 of culture, T cells were collected, washed and re-suspended in fresh medium. As basal level of HPSE release we used nonactivated T cells rested for 48–72 h in medium. Supernatant from $CD14^+$ monocytes and tumor cell lines were used as positive control. HPSE activity was determined as the inverse of decrease in absorbance as previously described[32,33]. T cell and tumor cell supernatants were analyzed in triplicate.

Multiplex for matrix metalloproteases (MMPs). Analysis of MMPs was performed using Milliplex Map kit panel 1 and 2 (Millipore) according to the manufacturer's instructions. In particular, FI-T cells were activated with OKT3 and anti-CD28 mAbs in presence of IL-2 (50 U/ml or 2000 U/ml) or IL-7 and IL-15 (10 ng/ml and 5 ng/ml, respectively). T cells were fed twice a week. At days 3, 7 and 10 of culture, supernatants and T cells were collected and 60 μg of sample were tested per well.

***p53* chromatin immunoprecipitation (ChIP) assay.** LTE-T cells, $CD45RA^+$ and $CD45RO^+$ T cells were collected and fixed with formaldehyde (Merck, Darmstadt, Germany) to a final concentration of 1%. Fixation proceeded at room temperature for 10 min and was stopped by the addition of glycine to a final concentration of 0.125 mol/liter. The cells were then washed twice

doi:10.1038/nm.3833

with cold PBS. Pellets were resuspended in 350 µl of lysis buffer and protease inhibitors mixture (Active Motif, Carlsbad, CA), washed and resuspended in 350 µl of optimized ChIP lysis buffer and protease inhibitors mixture (0.5% SDS, 10mM EDTA, 0.5 mM EGTA and 50 mM Tris-HCl, pH 8) and sonicated into chromatin fragments of an average length of 500 bp, as determined empirically by agarose gel electrophoresis of fragmented chromatin samples. Chromatin was kept at −80 °C. The chromatin solution was incubated with a *p53*-specific antibody that recognizes the full-length human protein (no. FL393, Santa Cruz) at 4 °C overnight with rotation. The immunoprecipitation was performed using Chip-IT Express kit (Active Motif, Carlsbad, CA) according to the manufacturer's instructions. Amplifications (37 cycles) were performed using specific primers (**Supplementary Fig. 11**), yielding PCR products ~200 bp in length (location of primers relatively to the origin of the promoter is indicated in parentheses after each primer pair). PCR products were separated by 1.5% agarose electrophoresis in Tris-borate-EDTA buffer and stained with ethidium bromide.

Retroviral constructs, transient transfection and transduction of T lymphocytes. *HPSE* cDNA (accession number NM_006665) was cloned into the SFG retroviral backbone that also encodes the GFP (SFG.HPSE(I)GFP) (**Supplementary Fig. 12**). The construct for the GD2-specific CAR containing the CD28, OX40 and ζ endodomains was previously described (SFG.CAR)[34]. We then generated a bicistronic vector to co-express the *HPSE* and CAR-GD2 using an IRES (SFG.CAR(I)HPSE) (**Supplementary Fig. 12**). The retroviral vector encoding the fusion protein GFP–firefly luciferase (GFP.FFLuc) for *in vivo* imaging of T cells and CD19-specific and CSPG4-specific CARs were previously described[35]. Transient retroviral supernatant was produced as previously described[35]. A specific inhibitor of HPSE, Roneparstat (SST0001) (a chemically modified heparin ^{100}Na,Ro-H, property of Sigma-tau Research Switzerland S.A.) (3 µg ml)[13,36,37], was added to the media during the virus preparation to increase its titer. Activated T lymphocytes were then transduced with retroviral supernatants using retronectin-coated plates (Takara Bio Inc., Shiga, Japan). After removal from the retronectin plates, T cell lines were maintained in complete T cell medium in a humidified atmosphere containing 5% CO_2 at 37 °C in the presence of IL-2 (50 U mL) for 2 weeks.

Flow cytometry. We performed flow cytometry analysis using the following antibodies: antibodies specific to CD45, CD56, CD8, CD4, CD3, CD45RA, CD45RO, CD62L, 7AAD and annexin V (all from Becton Dickinson, San Jose, CA) and CCR7 (from E&D) conjugated with FITC, PE, PerCP or APC fluorochromes. Expression of GD2 and CSPG4 antigens on tumor cell lines was assessed with anti-GD2 (clone 14.g2a, BD) and anti-CSPG4 (clone no. 1E6.4, Miltenyi-Biotec), respectively. The expression of GD2-specific CAR was detected using a specific anti-idiotype antibody (1A7). Samples were analyzed with a BD FACScalibur system equipped with a filter set for quadruple fluorescence signals and the CellQuest software (BD Biosciences). For each sample we analyzed a minimum of 10,000 events.

Chromium-release assay. The cytotoxic activity of T cells was evaluated using a standard 6-h ^{51}Cr-release assay.

Xenogenic mouse models. We used the NSG mouse model to assess the *in vivo* antitumor effect of control and transduced T cells. All mouse experiments were approved by the Institutional Animal Care and Use Committee of Baylor College of Medicine. 8–10-week-old male and female NSG mice (Jackson Laboratory, Bar Harbor, Maine) were injected i.p. with either CHLA-255 or LAN-1 neuroblastoma cells ($GD2^+$) (2.5×10^6) or SENMA melanoma cells ($CSPG4^+$) (5×10^5) resuspended in Matrigel (BD Biosciences). These tumor cell lines were labeled with Firefly luciferase. 10–12 d after neuroblastoma inoculation and 2 d after melanoma inoculation, LTE-T cells were injected i.p. (2×10^7 cells per mouse). No randomization was used. Investigators were not blinded, but mice were matched based on the signal of tumor cells before assignment to control or treatment groups. Mice were euthanized when signs of discomfort were detected by the investigator or as recommended by the veterinarian who monitored the mice three times a week. When valuable, tumor growth was also monitored by bioluminescence. For the *in vivo* biodistribution of T cells, 5×10^6 LTE-T cells per mouse labeled with the GFP.FFluc vector were infused via tail injection. For *in vivo* imaging, we used the Xenogen-IVIS Imaging System as previously described[35]. In the orthotopic model[26], an inoculum of 10^6 CHLA-255 luciferase-transduced tumor cells suspended in 0.1 ml of PBS was surgically implanted under the renal capsule of 5–7-week-old female mice using a 27-gauge needle. CAR^+ and $CAR(I)HPSE^+$ LTE-T cells were infused i.v. ($1–1.5 \times 10^7$ per mouse) 7 d later, and tumor regression was measured by bioluminescence imaging. By day 10, some mice were sacrificed and tumors collected, fixed and stained with anti-human CD3 mAb (no. A0452, Dako North America Inc., Carpinteria, CA). Mice were euthanized when signs of discomfort were detected by the investigator or as recommended by the veterinarian who monitored the mice three times a week or when luciferase signal reached 7.5×10^7 photons per second per cm^2 to investigate animal survival. For the lymphoma model, mice were infused i.v. with Daudi cells (2×10^6 cells) labeled with firefly luciferase. Four days later they were infused i.v. with 10^7 control or CAR^+ and $CAR(I)HPSE^+$ LTE-T cells specific for the CD19 antigen. Tumor growth was measured by bioluminescence imaging. Mice were euthanized when signs of discomfort were detected by the investigator or as recommended by the veterinarian who monitored the mice three times a week.

Tissue processing and immunohistochemistry. Tissue samples were fixed, processed and stained according to standard procedures. We performed H&E staining and labeling of human T cells using polyclonal rabbit anti-human CD3 mAb (A0452, Dako North America Inc., Carpinteria, CA) and for detection we used Dako LSAB + System-HRP (K0679, Dako). Tumors were scored without knowledge of the treatment used by the pathologist (M. Ittmann) by counting human infiltrating T lymphocytes in ten high-power fields at the edge of the tumor.

Statistical analyses. Unless otherwise noted, data are summarized as mean ± s.d. Student's *t*-test (two-sided) was used to determine statistically significant differences between samples, with $P < 0.05$ indicating a significant difference. When multiple comparison analyses were required, statistical significance was evaluated by a repeated-measures ANOVA followed by a log-rank (Mantel–Cox) test for multiple comparisons. The mouse survival data were analyzed using the Kaplan–Meier survival curve, and Fisher's exact test was used to measure statistically significant differences. Animals were excluded only in the event of their death after tumor implant but before T cell infusion. Neither randomization nor blinding was done during the *in vivo* study. However, mice were matched based on the tumor signal for control and treatment groups before infusion of control or gene modified T cells. When bioluminescence signal intensity was used to monitor tumor growth, values were log transformed and then compared using a two-sample *t*-test. In contrast, the analysis of the pathologist M. Ittmann, aimed at quantifying tumor infiltration by human T cells, was performed in a blinded fashion. We estimated the sample size considering the variation and mean of the samples. We tried to reach a conclusion using as small a sample size as possible. We estimated the sample size to detect a difference in means of 2 s.d. at the 0.05 level of significance with 80% power. Graph generation and statistical analyses were performed using Prism version 5.0d software (GraphPad, La Jolla, CA).

31. Yvon, E. *et al.* Immunotherapy of metastatic melanoma using genetically engineered GD2-specific T cells. *Clin. Cancer Res.* **15**, 5852–5860 (2009).
32. Roy, M. *et al.* Antisense-mediated suppression of Heparanase gene inhibits melanoma cell invasion. *Neoplasia* **7**, 253–262 (2005).
33. Zhang, L., Sullivan, P., Suyama, J. & Marchetti, D. Epidermal growth factor-induced heparanase nucleolar localization augments DNA topoisomerase I activity in brain metastatic breast cancer. *Mol. Cancer Res.* **8**, 278–290 (2010).
34. Pulè, M.A. *et al.* A chimeric T cell antigen receptor that augments cytokine release and supports clonal expansion of primary human T cells. *Mol. Ther.* **12**, 933–941 (2005).
35. Vera, J. *et al.* T lymphocytes redirected against the kappa light chain of human immunoglobulin efficiently kill mature B lymphocyte-derived malignant cells. *Blood* **108**, 3890–3897 (2006).
36. Naggi, A. *et al.* Modulation of the heparanase-inhibiting activity of heparin through selective desulfation, graded N-acetylation, and glycol splitting. *J. Biol. Chem.* **280**, 12103–12113 (2005).
37. Zhang, L., Ngo, J.A., Wetzel, M.D. & Marchetti, D. Heparanase mediates a novel mechanism in lapatinib-resistant brain metastatic breast cancer. *Neoplasia* **17**, 101–113 (2015).